ARTICLES
https://doi.org/10.1038/s41558-021-01000-1

nature climate change

Check for updates

Anthropogenic climate change has slowed global agricultural productivity growth

Ariel Ortiz-Bobea[1]✉, Toby R. Ault[2], Carlos M. Carrillo[2], Robert G. Chambers[3] and David B. Lobell[4]

Agricultural research has fostered productivity growth, but the historical influence of anthropogenic climate change (ACC) on that growth has not been quantified. We develop a robust econometric model of weather effects on global agricultural total factor productivity (TFP) and combine this model with counterfactual climate scenarios to evaluate impacts of past climate trends on TFP. Our baseline model indicates that ACC has reduced global agricultural TFP by about 21% since 1961, a slowdown that is equivalent to losing the last 7 years of productivity growth. The effect is substantially more severe (a reduction of ~26–34%) in warmer regions such as Africa and Latin America and the Caribbean. We also find that global agriculture has grown more vulnerable to ongoing climate change.

Enhancing agricultural productivity is vital to lifting global living standards and advancing sustainable food production in the face of escalating challenges to agriculture and the environment[1–7]. Investments in agricultural research have boosted agricultural productivity, but this growth in productivity has been distributed unequally across the world[8–10], and there are signs that it is slowing in certain regions[11–15]. At the same time, human activities during the last century and a half have caused global temperatures to rise by more than 1 °C above their pre-industrial values[16]. This increase affects the global weather patterns that are essential to agriculture[17,18]. However, the impacts of this ACC on the agricultural sector have not yet been quantified, as most research has focused on future impacts[19,20].

Research to date on the historical impact of ACC focuses overwhelmingly on yields of major cereal crops[21–23] or on total gross domestic product[24]. However, recent studies in this area are of limited value for assessing overall agricultural productivity for the following reasons: (i) cereal crops represent only about 20% of agriculture's global net production value (Extended Data Fig. 1), (ii) variations in measures such as yield, could deviate from changes in overall productivity if farmers also adjust inputs in response to weather[25–27] and (iii) growth and levels of total and agricultural GDP diverge considerably in most countries[28–30], and thus impacts of climate change on total GDP could deviate considerably from agricultural impacts[31,32]. There is much need for research on agricultural climate impacts beyond the effects on yields of the major staple crops[33].

We quantify the impact of ACC on global agricultural productivity since 1961 (ref. [34]). Instead of focusing on crop yield or agricultural output, we rely on a measure of agricultural TFP. TFP measures aggregate output per unit of measured aggregate input[35–38]. TFP thus captures interactions between output and input adjustments that eluded earlier research. Here we rely on official TFP statistics, for which agricultural output includes crops and livestock, while inputs encompass labour, land, physical capital and materials[12]. However, these TFP statistics do not incorporate the effect of weather.

Consider the production relation $Y_{it} = e^{f(Z_{it})} A_{it} X_{it} U_{it}$, where Y_{it} is aggregate agricultural output, $e^{f(Z_{it})}$ is the effect of weather Z_{it}, A_{it} measures technological knowledge and X_{it} and U_{it} are the observed and unobserved aggregate inputs, respectively. The subscripts refer to individual countries (i) and year (t). The percentage change in TFP is approximated as

$$\Delta \ln \mathrm{TFP}_{it} \equiv \Delta \ln(Y_{it}) - \Delta \ln(X_{it}) = \Delta \ln A_{it} + \Delta f(Z_{it}) + \Delta \ln U_{it},$$

where Δ denotes change. TFP growth reflects technological improvements embodied in $\Delta \ln A_{it}$ but also the unmeasured effects of random year-to-year weather changes $\Delta f(Z_{it})$ and unobserved input adjustments $\Delta \ln U_{it}$. While this aggregate representation may conceal fine-scale production processes that are important to practitioners in the field, it helps provide a much-needed macro-economic picture about the global agricultural economy.

We ground this conceptual framework empirically by estimating an econometric model linking country-level TFP growth with weather change. Our model characterizes f as a quadratic function of average temperature (T) and total precipitation (P) over the 5-month period centred around the greenest month of the year of each country or 'green season' (Methods):

$$\Delta \ln \mathrm{TFP}_{it} = \alpha_i + \theta_t + \beta_1 \Delta T_{it} + \beta_2 \Delta T_{it}^2 + \beta_3 \Delta P_{it} + \beta_4 \Delta P_{it}^2 + \epsilon_{it}.$$

Country-fixed effect α_i controls for average country TFP growth rates, and year-fixed effect θ_t for global shocks common to all nations. Conceptually, these parameters seek to control for technological change embodied in $\Delta \ln A_{it}$. Thus the β coefficients are estimated via the within-country and within-year variation of TFP growth and year-to-year weather changes. The inclusion of squared terms $\Delta(T_{it}^2)$ and $\Delta(P_{it}^2)$ allows the effect of changes in weather to vary with baseline levels of T or P. Unobserved changes in inputs that are not absorbed by α_i or θ_t and measurement errors in the TFP data are captured in the error term ϵ_{it}. Note that measurement error in the TFP data (Methods) that remain uncorrelated with year-to-year changes in weather do not introduce bias. We account for the uncertainty in the estimated parameters with a block bootstrap where we sample observations with replacement 500 times by year and region. We later consider more than 200 systematic

[1]Charles H. Dyson School of Applied Economics and Management, Cornell University, Ithaca, NY, USA. [2]Department of Earth and Atmospheric Sciences, Cornell University, Ithaca, NY, USA. [3]Department of Agricultural and Resource Economics, University of Maryland – College Park, College Park, MD, USA. [4]Department of Earth System Science and Center on Food Security and the Environment, Stanford University, Stanford, CA, USA. ✉e-mail: ao332@cornell.edu

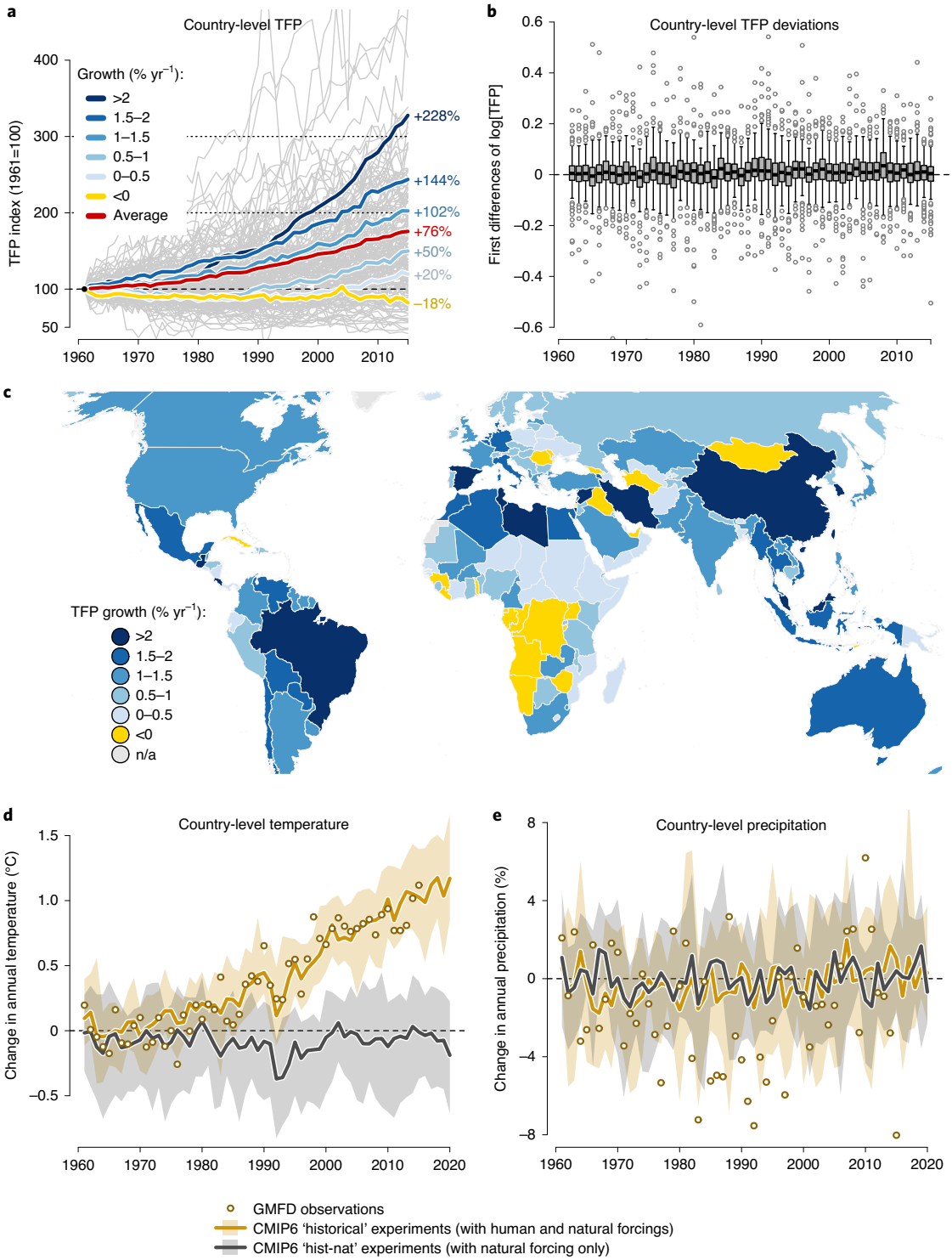

Fig. 1 | Recent trends in agricultural productivity and climate. a, Country-level growth in agricultural TFP over 1961–2015. Grey lines indicate observed TFP level trajectories for all countries in the sample. Coloured lines correspond to average TFP level trajectories for countries with varying average TFP growth rates. **b**, Distribution of first differences in the log of country-level TFP. The boxes represent the first three quartiles (Q1, Q2 and Q3). Whiskers extend to 1.5 times the interquartile range (IQR = Q3 – Q1). Observations falling beyond 1.5 IQR are represented with small circles. **c**, Map representing the annual average growth rate in agricultural TFP over 1961–2015. **d**,**e**, Evolution of global average annual temperature (**d**) and annual precipitation (**e**) of the Global Meteorological Forcing Dataset (GMFD) observations (circles). The golden band extends to the range of modelled variables from CMIP6 (seven GCMs). Simple averages of country-level variables are shown, thus small countries are over-represented.

variations of this model. For instance, we explore whether estimating separate response functions for various sub-regions of the world affects our results.

We summarize the key source data in Fig. 1. Figure 1a shows that average agricultural TFP has more than doubled since 1961 but that there is wide cross-country variation. Figure 1b shows that there is

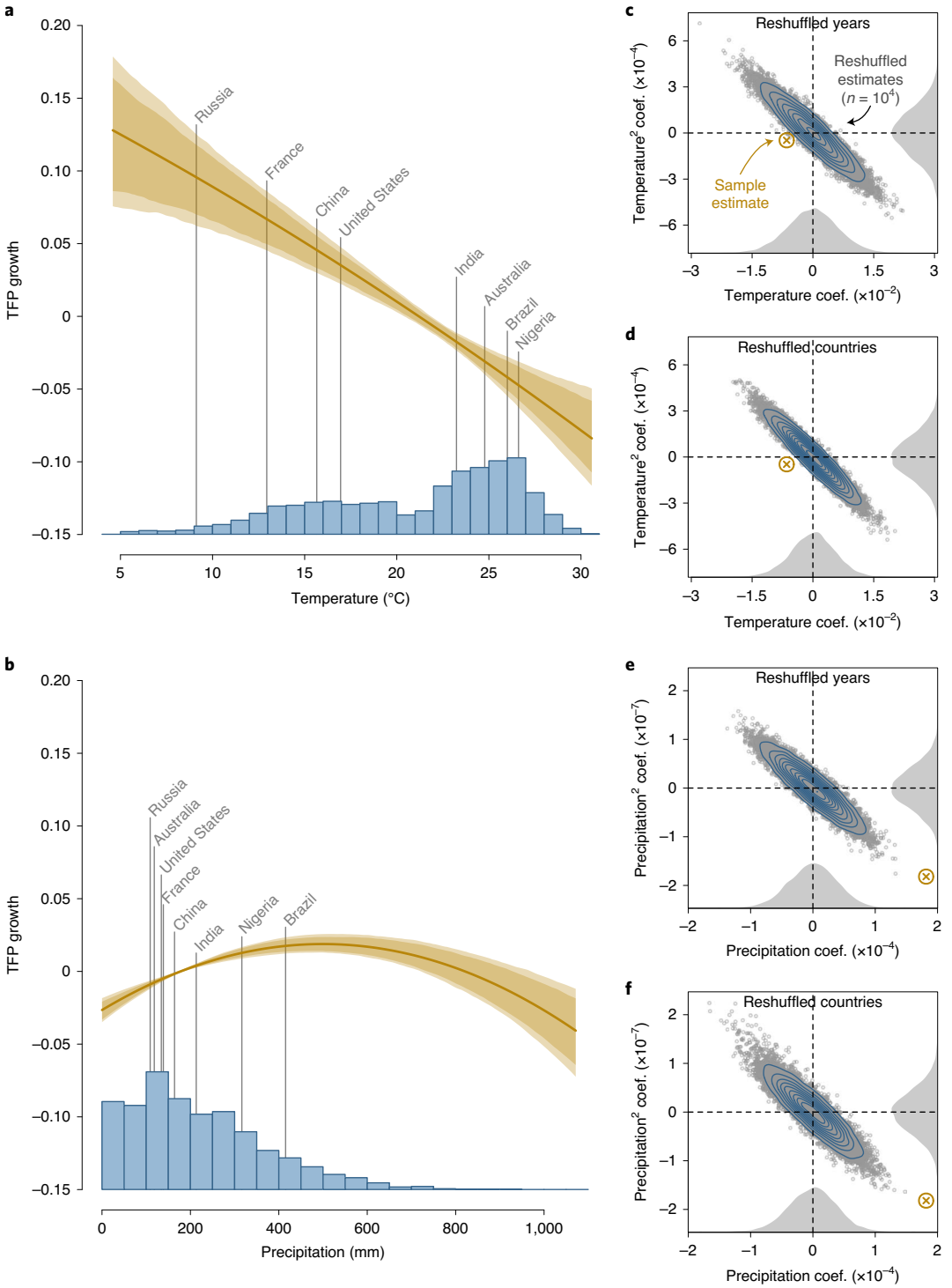

Fig. 2 | Response of agricultural productivity to weather. a,**b**, Response function of TFP growth to changes in green-season average *T* (**a**) and *P* (**b**). Response functions are centred vertically so that the exposure-weighted marginal effect is zero. The coloured bands represent 90% and 95% confidence bands based on 500 year-by-region block bootstraps. The blue bars represent the country-level distribution of green-season average *T* over the sample period 1962–2015. The average green-season *T* is indicated for a select number of large countries. **c**–**f**, Results of placebo checks whereby TFP and weather data are randomly mismatched or reshuffled by years (**c**,**e**) or country (**d**,**f**) where the distribution represents the linear and quadratic *T* (**c**,**d**) or *P* (**e**,**f**) coefficients based on 10,000 reshuffled datasets.

a substantial range of variation in $\Delta \ln \mathrm{TFP}_{it}$ across countries for any given year. We also observe that TFP has grown much more slowly in certain countries, particularly in Sub-Saharan Africa (Fig. 1c). Figure 1d shows how observed annual country-level average temperatures (in circles) fall closer within the range of counterfactual weather trajectories with ACC (gold band) than without ACC (grey band). Figure 1e shows analogous information for precipitation without any discernible pattern.

We find a robust relationship between agricultural TFP growth and weather changes (Fig. 2 and Supplementary Table 1).

The temperature response function is roughly linear and downward sloping (Fig. 2a), indicating that warmer temperatures over the green season are detrimental to TFP growth. We conduct two placebo checks that suggest this relationship is unlikely to arise by chance. These checks are based on the idea that incorrectly matching TFP growth and weather changes, and re-estimating, should yield results suggesting no or insignificant effects of weather on TFP. We first estimate models based on 10,000 'reshuffled' datasets that mismatch the year variable of the TFP growth and weather change data. The sample estimate (Fig. 2a) falls outside the resulting distribution of spurious 'reshuffled estimates' (Fig. 2c). In a second check, we mismatch the country variable of the TFP growth and weather change data, with similar results (Fig. 2d). The precipitation response function is non-linear and peaks at around 500 mm over the green season (Fig. 2b). We demonstrate that this relationship is not likely spurious with the same placebo checks shown in Fig. 2e,f. We also find that the shape of the response functions is not driven by either hot or cold countries (Supplementary Figs. 1 and 2).

A critical question for climate change adaptation is whether agriculture is becoming more or less sensitive to climatic extremes. This would be reflected empirically as changes over time in the response functions shown in Fig. 2. We estimate a model based on the first (1962–1988) and second (1989–2015) halves of the sample and find that the temperature response function is noticeably steeper for the latter half (Supplementary Figs. 4 and 5). This indicates that higher temperatures have become more damaging. We formally confirm this by testing whether the temperature coefficient has changed between these two periods in a model with a linear specification for temperature ($P=0.035$). We also find that the change in the temperature response function over time is not driven by isolated changes in outlying countries in the temperature distribution (Supplementary Figs. 6–9). Note that, because the response functions are roughly flat for models based on early, 1962–1988 data, the coefficients do not fall outside the distribution of 'reshuffled' estimates in Supplementary Figs. 4b,c, 6b,c and 8b,c. This mirrors recent findings in US agriculture[39,40].

We find no evidence that weather has a persistent effect on TFP growth. Our baseline specification only considers contemporaneous weather effects. But a weather shock could conceivably affect TFP growth in future years, for example, if growth is faster following a year with bad weather. This would result in cumulative weather events affecting TFP growth. By introducing lags for weather in prior years, we cannot reject the hypothesis that the cumulative effect of changes in weather conditions up to 10 years in the past have no effect on TFP growth (Supplementary Table 2). But rejecting this hypothesis may be challenging with aggregate data.

We subsequently link our econometric estimates with counterfactual weather trajectories from climate experiments with and without ACC to derive the cumulative impact of ACC for each country since 1961. We obtain the counterfactual weather trajectories from the Coupled Model Intercomparison Project Phase 6 (CMIP6). This approach combines both the statistical uncertainty from the econometric model regarding the climate–agriculture relationship and the climate uncertainty from the CMIP6 ensemble regarding the effect of human emissions on the climate system (Methods).

The cumulative impact of ACC on global agricultural TFP growth over the 1961–2020 period is about −20.8% with a 90% confidence interval between −39.1% and −10.1% (Fig. 3a). Figure 3b shows this finding in levels by combining the counterfactual cumulative impacts of ACC on global TFP growth with the observed (1961–2015) and projected (2016–2020) global TFP level trajectory. This illustrates how much higher global TFP would have been without ACC. Specifically, we find that the global TFP level projected to be reached in 2020 in our world with ACC would have been reached in 2013 in a world without ACC, with a 90% confidence interval between 2007 and 2016. That is, the impact of ACC represents a loss of the past 7 years of productivity growth.

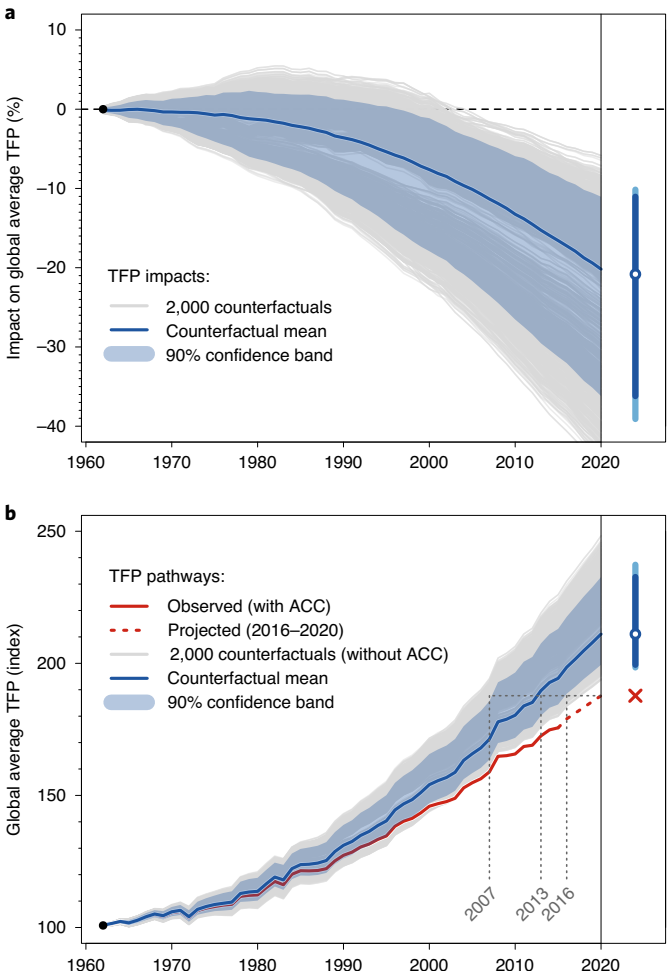

Fig. 3 | Global impact of ACC on productivity. a, A total of 2,000 counterfactual pathways combining statistical uncertainty and climate uncertainty. The blue line shows ensemble mean, and the blue cone represents a 90% confidence band. The error bars on the right indicate 90% and 95% confidence intervals for the impact on 2020. **b**, Same results presented in levels relative to the observed (1962–2015) and projected (2016–2020) level of TFP (in red).

Our baseline global finding of the impact of ACC on global agricultural productivity is robust to a wide range of specifications of the econometric model. Figure 4 summarizes global estimates for the baseline and a subset of alternative models (96). Extended Data Fig. 10 summarizes global estimates for an even wider range of specifications (298). The baseline model is shown in blue in Fig. 4 and corresponds to the estimate shown in Fig. 3a. Notice that using minimum (T_{min}) and maximum (T_{max}) temperature as alternative temperature variables does not substantially change our baseline estimate. Extended Data Fig. 10 shows that excluding precipitation also does not change results substantially. In addition, using a cubic functional form to relax the symmetry of our baseline quadratic specification does not alter our baseline result. We also consider regressions with observations weighted by revenue and find those results to be systematically more pessimistic than our baseline model using equal weights. Aggregating weather data to country level on the basis of areas covered only by cropland or both cropland and pasture has little effect on our findings. We also consider models with weather variables aggregated over the entire calendar

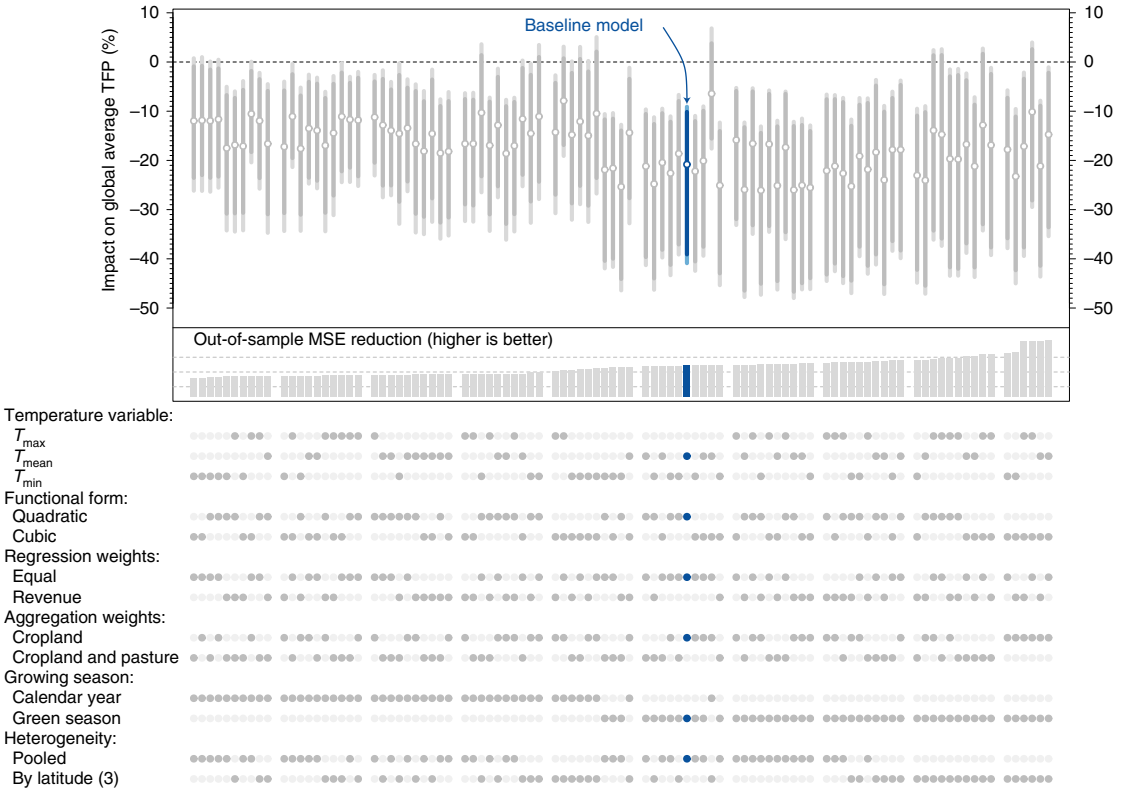

Fig. 4 | Global impact of ACC for multiple econometric models. Impact estimates for 96 model variations, where lines indicate 90% (dark) and 95% (light) confidence intervals around the ensemble mean estimate for a particular model for the baseline model (Fig. 3a, blue) and alternative models (grey). Vertical bars directly below represent the reduction in out-of-sample MSE of tenfold cross-validation (whereby years of data are sampled together) relative to a model that excludes weather variables, thus higher bars indicate better model fit. The dots provide information about the characteristics of each econometric model shown above.

year and find that those models fit less well and point to noticeably smaller damage. We also consider a model based on two seasons, a 3-month 'green' season and a 3-month 'brown' (or dry) season (Methods). Results shown in Extended Data Fig. 10 indicate that this does not substantially improve model fit or affect impact estimates in a meaningful way. Finally, our baseline model imposes a single response function for the whole world. But allowing separate response functions for three equally sized latitudinal groups of countries does not alter our findings. Overall, the 288 models that do not exclude observations point to an average mean impact of −16.9% with a standard deviation of 5.9% (indicated with a horizontal red line and band in Extended Data Fig. 10).

The exclusion of certain countries does not substantially affect our baseline estimate, but restricting the analysis to certain temporal subsamples does. A potential concern is that certain countries may overinfluence our estimates and thus drive our findings. But excluding certain large countries such as China, the United States, India or Brazil, the 10% coldest or hottest countries or the 10% or 20% smallest countries (by average agricultural revenue) does not substantially alter our baseline finding (Extended Data Fig. 10). However, basing our analysis on the latter part of the sample (1989–2015) points to even larger damage than our baseline estimate, on the order of −30% (Extended Data Fig. 10). This reflects our finding that the response function is changing over time and suggests that global agriculture is growing increasingly sensitive to ongoing climate change.

Our global results conceal sizeable regional and cross-country disparities. Figure 5 shows that the cumulative impact of ACC since 1961 is greater for warm regions such as Africa (−34.0%), the Near East and North Africa (−30.0%) and Latin American and the Caribbean (−25.9%) than for cooler regions such as North America (−12.5%) and Europe and Central Asia (−7.1%) (Supplementary Table 3). Importantly, these regional impacts are constructed by weighting econometric models based on how well they fit the data, so results reflect the econometric model uncertainty (Methods). The large negative impacts for Africa seem particularly worrisome given the large portion of the population employed in agriculture. Overall, these findings are consistent with some localized slowdowns in agricultural productivity growth[11–15], but also with studies analysing economy-wide ACC impacts that exacerbate inequality between poor and rich countries[24,41]. The most affected areas include regions with low agricultural productivity such as Sub-Saharan Africa[42,43].

Finally, we find that ignoring input responses, by analysing output rather than TFP, makes global impacts of ACC appear more severe. The temperature response function is steeper for output than for TFP (Supplementary Fig. 1), suggesting that farmers reduce aggregate input quantity in response to detrimental weather conditions. That is, weather effects on output reflect direct effects on production, but also indirect effects via weather-induced reductions in inputs. Such indirect input effects are not captured by the TFP model. Ignoring confounding input adjustments, Supplementary Fig. 2 indicates that ACC would have reduced output by about 27.6% with a 90% confidence interval between −48.3% and −14.3%. This is noticeably higher than the 20.8% reduction based on TFP.

Our estimates should not be interpreted as the effect of a world without fossil fuels on global agricultural production. Agriculture has benefitted tremendously from agricultural research and carbon-intensive inputs that would not have been as available without fossil fuels. The counterfactual in our study only removes the effect that fossil fuels and other anthropogenic influences have on

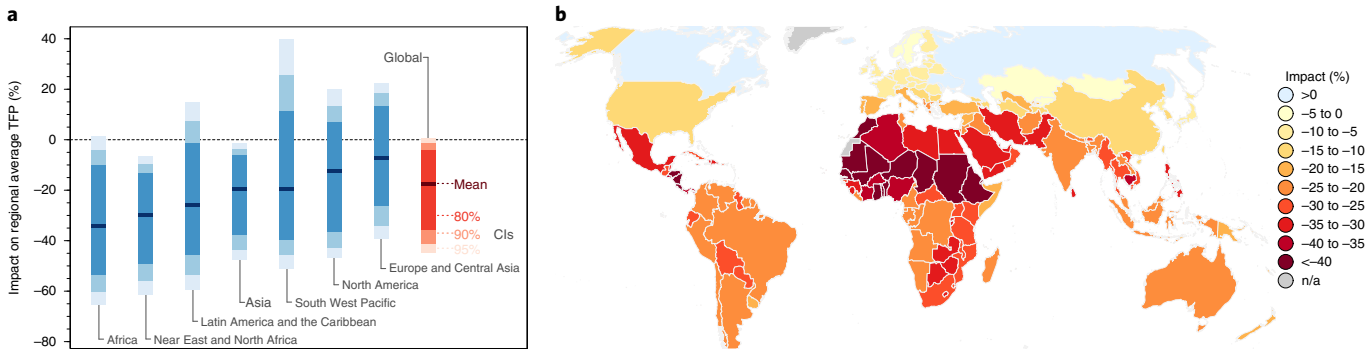

Fig. 5 | Global, regional and country-level impacts of ACC. a, Impact estimates for each region reflecting various sources of uncertainty. The coloured bands represent 95%, 90% and 80% confidence intervals (CIs) that reflect climate uncertainty (from GCMs), econometric uncertainty (from the estimation) and specification uncertainty (from the choice of the econometric model) (Methods). **b**, The colour in the map corresponds to the ensemble mean impact for each country based on these three sources of uncertainty.

the climate system. For instance, our estimates do not remove the direct effect that rising CO_2 concentrations have on agricultural production or the presence of agricultural research or carbon-intensive inputs. In addition, the reader may be rightfully concerned about measurement error of our TFP metric. TFP estimates are notoriously difficult to construct and require considerable background work, sometimes using imperfect data sources. However, as long as the measurement error remains uncorrelated with year-to-year changes in TFP growth, which seems plausible, such errors do not bias our econometric estimates but simply render them more imprecise. Moreover, the TFP metric we rely upon likely mismeasures certain inputs, such as irrigation water use. Our own analysis shows that ignoring all measured inputs overstates ACC impacts, so the present analysis is a first step while more detailed international TFP statistics are produced. In conclusion, our study suggests that ACC is increasingly reducing agricultural output as we drift away from a climate system without human influences, cumulating into a detectable and sizeable impact as of 2020. Given recent localized productivity slowdowns[11–15], the long lags in agricultural research and the rapid pace of ACC, our findings raise the question of whether current levels of investments in agricultural research are sufficient to sustain twentieth-century rates of productivity growth in the twenty-first century.

Online content

Any methods, additional references, Nature Research reporting summaries, source data, extended data, supplementary information, acknowledgements, peer review information; details of author contributions and competing interests; and statements of data and code availability are available at https://doi.org/10.1038/s41558-021-01000-1.

Received: 28 August 2020; Accepted: 2 February 2021;
Published online: 1 April 2021

References

1. Johnston, B. F. & Mellor, J. W. The role of agriculture in economic development. *Am. Econ. Rev.* **51**, 566–593 (1961).
2. Timmer, C. P. The agricultural transformation. *Handb. Dev. Econ.* **1**, 275–331 (1988).
3. Barrett, C. B., Carter, M. R. & Timmer, C. P. A century-long perspective on agricultural development. *Am. J. Agric. Econ.* **92**, 447–468 (2010).
4. de Janvry, A. & Sadoulet, E. Agricultural growth and poverty reduction: additional evidence. *World Bank Res. Observer* **25**, 1–20 (2010).
5. Christiaensen, L., Demery, L. & Kuhl, J. The (evolving) role of agriculture in poverty reduction-An empirical perspective. *J. Dev. Econ.* **96**, 239–254 (2011).
6. *World Development Report 2008: Agriculture for Development* (World Bank, 2007); https://openknowledge.worldbank.org/handle/10986/5990
7. Curtis, P. G., Slay, C. M., Harris, N. L., Tyukavina, A. & Hansen, M. C. Classifying drivers of global forest loss. *Science* **361**, 1108–1111 (2018).
8. Steensland, A. *2019 Global Agricultural Productivity Report: Productivity Growth for Sustainable Diets and More* (Virginia Tech, 2019); http://hdl.handle.net/10919/96429
9. *2020 Global Food Policy Report: Building Inclusive Food Systems* (International Food Policy Research Institute, 2020); https://doi.org/10.2499/9780896293670
10. Fuglie, K. R. Capital, R&D spillovers, and productivity growth in world agriculture. *Appl. Econ. Perspect. Policy* **40**, 421–444 (2018).
11. Alston, J. M., Beddow, J. M. & Pardey, P. G. Agricultural research, productivity, and food prices in the long run. *Science* **325**, 1209–1210 (2009).
12. Fuglie, K. O., Wang, S. L. & Ball, V. E. (eds) *Productivity Growth in Agriculture: an International Perspective* (CABI, 2012).
13. Fuglie, K. O. Is agricultural productivity slowing? *Glob. Food Secur.* **17**, 73–83 (2018).
14. Ball, E. V., San Juan, C., Sunyer Manteiga, C. & Sheng, Y. Technology catch-up in agriculture among advanced economies. Working Paper Economics 20-03 (Universidad Carlos III de Madrid, 2020).
15. Chambers, R. G., Pieralli, S. & Sheng, Y. The millennium droughts and Australian agricultural productivity performance: a nonparametric analysis. *Am. J. Agric. Econ.* **102**, 1383 (2020).
16. IPCC *Climate Change 2014: Synthesis Report* (eds Core Writing Team, Pachauri, R. K. & Meyer L. A.) (IPCC, 2014).
17. Lesk, C., Rowhani, P. & Ramankutty, N. Influence of extreme weather disasters on global crop production. *Nature* **529**, 84–87 (2016).
18. Ray, D. K., Gerber, J. S., MacDonald, G. K. & West, P. C. Climate variation explains a third of global crop yield variability. *Nat. Commun.* **6**, 1–9 (2015).
19. Zhao, C. Temperature increase reduces global yields of major crops in four independent estimates. *Proc. Natl Acad. Sci. USA* **114**, 9326–9331 (2017).
20. Liu, B. Similar estimates of temperature impacts on global wheat yield by three independent methods. *Nat. Clim. Change* **6**, 1130–1136 (2016).
21. Lobell, D. B. & Field, C. B. Global scale climate–crop yield relationships and the impacts of recent warming. *Environ. Res. Lett.* **2**, 014002 (2007).
22. Lobell, D. B., Schlenker, W. & Costa-Roberts, J. Climate trends and global crop production since 1980. *Science* **333**, 616–620 (2011).
23. Moore, F. C. The fingerprinting of anthropogenic warming on global agriculture. Preprint at *Earth arXiv* https://doi.org/10.31223/X5Q30Z (2020).
24. Diffenbaugh, N. S. & Burke, M. Global warming has increased global economic inequality. *Proc. Natl Acad. Sci. USA* **116**, 9808–9813 (2019).
25. Kaufmann, R. K. & Snell, S. E. A biophysical model of corn yield: integrating climatic and social determinants. *Am. J. Agric. Econ.* **79**, 178–190 (1997).
26. Jagnani, M., Barrett, C. B., Liu, Y. & You, L. Within-season producer response to warmer temperatures: defensive investments by Kenyan farmers. *Econ. J.* **131**, 392–419 (2020).
27. Aragón, F. M., Oteiza, F. & Rud, J. P. Climate change and agriculture: subsistence farmers' response to extreme heat. *Am. Econ. J. Econ. Policy* **13**, 1–35 (2021).
28. Schultz, T. W. *Transforming Traditional Agriculture* (Yale Univ. Press, 1964).
29. Gollin, D., Lagakos, D. & Waugh, M. E. The agricultural productivity gap. *Q. J. Econ.* **129**, 939–993 (2014).
30. Adamopoulos, T. & Restuccia, D. The size distribution of farms and international productivity differences. *Am. Econ. Rev.* **104**, 1667–1697 (2014).
31. Dell, M., Jones, B. F. & Olken, B. A. Temperature shocks and economic growth: evidence from the last half century. *Am. Econ. J.: Macroecon.* **4**, 66–95 (2012).
32. Burke, M., Hsiang, S. M. & Miguel, E. Global non-linear effect of temperature on economic production. *Nature* **527**, 235–239 (2015).

33. Hertel, T. W. & de Lima, C. Z. Climate impacts on agriculture: searching for keys under the streetlight. *Food Policy* **95**, 101954 (2020).
34. Ortiz-Bobea, A. et al. Replication files for anthropogenic climate change has slowed global agricultural productivity growth. Version 2 (Cornell Institute for Social and Economic Research, 2021); https://doi.org/10.6077/pfsd-0v93
35. Comin, D. In *Economic Growth* (eds Durlauf, S. N. & Blume, L. E.) 260–263 (Palgrave Macmillan, 2010).
36. Hulten, C. R. In *New Developments in Productivity Analysis* (eds Hulten, C. R. et al.) 1–54 (Univ. Chicago Press, 2001).
37. Van Beveren, I. Total factor productivity estimation: a practical review. *J. Econ. Surv.* **26**, 98–128 (2012).
38. Coomes, O. T., Barham, B. L., MacDonald, G. K., Ramankutty, N. & Chavas, J. P. Leveraging total factor productivity growth for sustainable and resilient farming. *Nat. Sustain.* **2**, 22–28 (2019).
39. Liang, X.-Z. et al. Determining climate effects on US total agricultural productivity. *Proc. Natl Acad. Sci. USA* **114**, E2285–E2292 (2017).
40. Ortiz-Bobea, A., Knippenberg, E. & Chambers, R. G. Growing climatic sensitivity of US agriculture linked to technological change and regional specialization. *Sci. Adv.* **4**, eaat4343 (2018).
41. Letta, M. & Tol, R. S. J. Weather, climate and total factor productivity. *Environ. Resour. Econ.* **73**, 283–305 (2019).
42. Frisvold, G. & Ingram, K. Sources of agricultural productivity growth and stagnation in sub-Saharan Africa. *Agric. Econ.* **13**, 51–61 (1995).
43. Fuglie, K. & Rada, N. *Resources, Policies, and Agricultural Productivity in sub-Saharan Africa.* USDA-ERS Economic Research Report No. 145 (United States Department of Agriculture, 2013).

Methods

Data sources and data processing. We obtain agricultural data from the United States Department of Agriculture (USDA) Economic Research Service (ERS) International Agricultural TFP dataset[44]. This dataset provides the most comprehensive set of international TFP estimates for the agricultural sector. The dataset provides country-level TFP indices (in levels) for 172 countries over the 1961–2015 period. The regression dataset has 9,255 observations with 172 countries and 54 years (1962–2015; note that one year is lost because of first differencing to compute growth rates). The dataset is balanced but for one nation, Palestine, for which we only have complete data from 1995. Note that some recent smaller nations were aggregated to their former larger countries to extend the time span of the dataset (for example, Czechoslovakia, Yugoslavia, Ethiopia, Sudan, etc.).

TFP levels, annual growth rates and average growth rates are shown in Fig. 1a–c. The TFP growth rate for country i and year t is constructed by the USDA as

$$\Delta \ln \mathrm{TFP}_{it} = \sum_j R_{itj} \ln \Delta Y_{itj} - \sum_k S_{itk} \ln \Delta X_{itk},$$

where R_{itj} is the revenue share of the jth output Y_{itj} and S_{itk} is the cost share of the kth input X_{itk}. As indicated by the USDA, TFP growth is the value-share-weighted difference between total output growth and total input growth. To avoid index number bias, the USDA adjusts weights R_{itj} and S_{itk} every decade. As indicated in ref. [45], this expression for TFP growth is derived from farmer profit-maximizing behaviour with an underlying Cobb–Douglas production function exhibiting constant returns to scale. Thus, changes in R_{itj} and S_{itk} every decade essentially reflect changes in output elasticities of inputs in the underlying production function over time within each country.

Outputs include crop and livestock commodities aggregated based on a common set of international prices derived by the Food and Agriculture Organization (FAO). Inputs include farm labour, agricultural land (quality adjusted), capital inputs (including farm machinery and livestock) and intermediate inputs (inorganic fertilizer and animal feed) which are mostly obtained from the FAO. Thus changes in inventory in livestock herd size are taken into account. See ref. [45] for more details. Note that, although the data are constructed in terms of TFP growth rates, the data are transformed and reported in levels on the USDA website. Geographical delimitations in this study follow as close as possible FAO region definitions (Supplementary Fig. 3). Note that the TFP metric we rely upon likely mismeasures certain inputs, such as irrigation water use. As discussed in ref. [45], irrigation is accounted for in the land input through a quality adjustment of land equipped for irrigation. Thus changes in irrigation intensity remain unaccounted for. However, estimates of weather-driven variability in global irrigation withdrawals remain modest at a global scale (~10%)[46]. We obtain regional or global TFP growth rates by computing revenue-weighted averages of country-level TFP growth rates. We use a constant revenue weight based on average revenue over the 1961–2015 period to simplify our interpretations. Note this approach differs slightly from the USDA approach, which consists of deriving regional or global TFP growth rates from aggregate regional or global outputs and inputs (using revenue and cost shares that vary by decade). Results remain fairly similar. For instance, our approach indicates a global TFP increase of 76% over 1961–2015 whereas the USDA indicates a 71% rise.

We obtain the historical weather data from the Global Meteorological Forcing Dataset (GMFD) for land surface modelling developed by the Terrestrial Hydrology Research Group at Princeton University[47]. The GMFD provides data on daily minimum and maximum temperature and total precipitation over 1948–2016 with a 0.25° spatial resolution (~28 km at the Equator). Following standard practice in the literature, we aggregate these variables to the monthly level and then spatially aggregate the grids to the country level based on either cropland or cropland and pasture weights. We obtain these weights by resampling the 10-km gridded land cover data in ref. [48] to the GMFD grid using bilinear interpolation (Supplementary Fig. 4). Although weighting weather data by production value may seem desirable, we find that (1) adopting alternative weighting schemes makes little practical difference, and (2) constructing a globally consistent set of grid-level production value weights would be prohibitive. We show the annual evolution of the country-level average temperature and percentage change in total precipitation for the 1961–2015 period in Fig. 1d,e.

We obtain the counterfactual monthly weather trajectories for average temperature and total precipitation for 1961–2020 from three sets of simulations in CMIP6. The 'hist-nat' experiment (1961–2020) simulates the influence of natural forcing alone on the climate system. The 'historical' experiment (1961–2014) simulates the influence of both human and natural forcings on the climate system. As stipulated by CMIP6, we complement this experiment with data for 2015–2020 from the SSP2–4.5 experiment. We rely on seven general circulation models (GCMs) (Supplementary Table 4).

To aggregate these modelled weather trajectories to the country level using the same approach as above, we first downscale these data from their native GCM grid to the GMFD grid using the bias-corrected spatial disaggregation (BCSD) approach[49]. BCSD corrects the bias of the modelled climate data and increases the spatial resolution with the ultimate goal of having a product of higher resolution that conserves the statistics of the global climate scenarios. The BCSD approach is performed in two steps. In the first step, we create a bias-corrected (BC) dataset by performing a quantile mapping to correct the bias[50,51], which ref. [52] calls a 'transformation'. In the quantile mapping, we transform the GCM time series field to match the quantile distribution of the observed GMFD weather dataset, $Q_{GCM} \rightarrow Q_{OBS}$, using a common period for the transformation function (1961–2014). Because the transformation is done at every grid cell of the GCM, the observed GMFD dataset was aggregated to match the coarser GCM resolution. The approach was applied to both temperature and precipitation. In the second step, we increased the spatial resolution of the BC data by applying the spatial disaggregation (SD) approach. In the SD approach, we first removed the monthly observed climatology from the coarse resolution BC data, $\Delta F = F - \mathrm{CLIM}_{\mathrm{COARSE}}$. We then convert the anomaly to a high resolution by linear interpolation, $\Delta F \rightarrow \Delta F_{\mathrm{HIGH}}$. Finally, we added the climatology with high resolution, $F_{\mathrm{HIGH}} = \Delta F_{\mathrm{HIGH}} + \mathrm{CLIM}_{\mathrm{HIGH}}$. Here, the anomaly calculation (ΔF) is only valid for temperature. For precipitation, the anomaly is computed using a ratio, $\Delta F = F/\mathrm{CLIM}_{\mathrm{COARSE}}$ with $F_{\mathrm{HIGH}} = \Delta F_{\mathrm{HIGH}} \times \mathrm{CLIM}_{\mathrm{HIGH}}$.

The baseline econometric model relies on weather variables aggregated over the 'green season', a 5-month period centred around the greenest month of year of each country based on normalized difference vegetation index (NDVI) climatology data[53]. The motivation behind the green season is to avoid incorporating periods of the year with relatively little vegetation growth which are critical both for crop and livestock production. We also consider a series of models with two seasons, a 3-month 'green' season and a 3-month 'brown' (dry) season, each centred around the highest and lowest NDVI value, respectively. The NDVI data is the third generation of the National Aeronautics and Space Administration/Goddard Space Flight Center Global Inventory Modeling and Mapping Studies NDVI dataset for 1981–2015. We first temporally aggregate the data to bi-weekly climatologies. We then smooth the climatology series within the year based on a 14-week moving window. We then identify the 'greenest' month based on the month that includes the highest NDVI level of the year for each grid cell. The spatial distribution of the 'greenest' month for each grid cell is shown in Supplementary Fig. 5. To obtain a country-level value, we first resample land cover weights to match that of the NDVI data. We then compute for each country the most frequent 'greenest' and 'least green' months based on either cropland or cropland and pasture frequency weights. These country-level aggregations are shown in Supplementary Fig. 5. For two small island nations (Fiji and Polynesia) there are no NDVI data. We therefore assign the greenest and least green months to match that of the neighbouring island nation of Vanuatu.

Deriving the response function. To help map our conceptual framework to the USDA TFP estimates, we consider the following relationship between aggregate output, aggregate input, weather and technological knowledge $Y_{it} = e^{f(Z_{it})} A_{it} X_{it} U_{it}$, where Y_{it} is aggregate agricultural output in country i and year t, $e^{f(Z_{it})}$ is the effect of weather Z_{it}, A_{it} measures current technological knowledge and X_{it} and U_{it} are observed and unobserved aggregate inputs, respectively. By definition, TFP for country i at time t is Y_{it}/X_{it}, so that the percentage change in TFP for country i at time t is approximated as

$$\Delta \ln \mathrm{TFP}_{it} \equiv \Delta \ln(Y_{it}) - \Delta \ln(X_{it}) = \Delta \ln A_{it} + \Delta f(Z_{it}) + \Delta \ln U_{it}.$$

Empirically, our econometric models seek to control for $\Delta \ln A_{it}$ through country and year fixed effects (α_i and θ_t, respectively) and model $\Delta f(Z_{it})$ in various ways. Because the model is specified in growth terms, the inclusion of a country-specific dummy variable α_i is analogous to controlling for a linear country-specific time trend in ln TFP. Unobserved inputs that are not absorbed by the fixed effects are captured in the error term ϵ_{it}. This error term also captures measurement errors in the TFP metric, which includes changes in irrigation water use not fully captured by changes in irrigated area. Perhaps with the exception of water withdrawals, measurement errors in the TFP data are unlikely to be correlated with year-to-year weather changes, which does not bias our results. Our baseline model regresses $\Delta \ln \mathrm{TFP}_{it}$ on first differences of green-season average temperature and precipitation:

$$\Delta \ln \mathrm{TFP}_{it} = \beta_1 \Delta T_{it} + \beta_2 \Delta T_{it}^2 + \beta_3 \Delta P_{it} + \beta_4 \Delta P_{it}^2 + \alpha_i + \theta_t + \epsilon_{it}.$$

To capture the statistical uncertainty of the regression model, we conduct a block bootstrap estimation where we sample observations by year–region with replacement. While there is serial dependence in TFP levels, previous work has shown there is no serial dependence in growth $\Delta \ln \mathrm{TFP}_{it}$ (for example, refs. [14,37]). We thus focused on accounting for contemporaneous regional dependence. Regions correspond to the seven FAO regions shown in Supplementary Fig. 3. We show the response function with a 90% bootstrapped confidence band for temperature and precipitation in Fig. 2a,b. We show regression coefficients for the baseline model in Supplementary Table 1. Weather parameters β are subsequently used in a simulation to derive the effect of ACC on global agricultural TFP. Importantly, note that measurement error in $\Delta \ln \mathrm{TFP}_{it}$ would need to be correlated with ΔT_{it} and/or ΔP_{it} to induce any form of bias in the estimation of $\hat{\beta}$. In addition, classical measurement error in ΔT_{it} and/or ΔP_{it} would induce attenuation bias, reducing the magnitude of our findings.

The placebo checks shown in Fig. 2c–f evaluate whether the estimated relationship is spurious. The idea is to evaluate the chances that the result is spurious

by contrasting the estimated coefficients in our sample with a distribution of coefficients from 'reshuffled' datasets where we should, on average, expect no effect of weather. We perform 10,000 regressions based on datasets that are mismatched by year and by country. In all cases the estimated coefficients fall clearly outside the distribution of 'reshuffled' estimates, in support of our baseline model.

Robustness checks. A crucial concern in applied econometric analysis is that baseline models proposed by researchers may not be robust to even small variations in model specification or the underlying data. We conduct a systematic exploration spanning 296 variations of the econometric model to assess the robustness of our baseline finding (Extended Data Fig. 10). The upper part of the figure shows the cumulative impact of ACC on global agricultural TFP since 1961 for each one of these model variations. Each point and associated confidence bands corresponds to a particular model. The lower part of the figure shows the characteristics of each model in a dotted table. The baseline model, which corresponds to the impact estimate shown on the right in Fig. 3a, is highlighted in blue. Note that Fig. 4 shows a subset of the models in the main text.

We consider all possible combinations of models along the following dimensions: (1) relies on either T_{max}, T_{min} or T_{mean}, (2) includes or excludes precipitation, (3) adopts a quadratic or cubic functional form for all weather variables, (4) relies on equal or revenue regression weights, (5) relies on weather data aggregated over cropland or cropland and pasture, (6) relies on the calendar year, the 'green season' (5 months centred around the greenest month) for aggregating weather conditions or two 3-month long 'green' and 'brown' seasons and (7) relies on a single global response function or on separate response functions for three equally sized latitudinal regions. This corresponds to $3\times2\times2\times2\times2\times3\times2=288$ variations of the model which are codified in the bottom part of Extended Data Fig. 10. For instance, the dotted table in Extended Data Fig. 10 indicates that the baseline model (shown in blue) adopts T_{mean} as the temperature variable, includes precipitation in the specification, assumes a quadratic response function, relies on equal regression weights, is based on regression data aggregated over cropland areas, is based on weather variables constructed over the 'green season', assumes a singled 'pooled' global response function and does not exclude any observations.

We find that most of these variations have relatively little bearing on the baseline result presented in Fig. 3. The adoption of revenue regression weights and a 'green season' for weather aggregation represent the two most consequential modeling choices, pointing to slightly larger damage. Overall, we find that these models tend to better fit the data. Restricting weather variables to the greenest months may reduce measurement error of relevant weather conditions. Similarly, it is possible that smaller countries may have noisier agricultural data, so downweighting them in the regression or excluding them from the models improves model fit. In addition, note that alternative regression weights may signal unmodelled heterogeneity in the response function[54], suggesting that smaller countries in our sample may appear slightly less sensitivity to weather than larger nations.

We also consider ten data restrictions including country exclusions (China, the United States, India, Brazil, coldest 10%, hottest 10% and smallest 10% and 20%) and temporal subsets (1962–1988 and 1989–2015) which are discussed in the main paper. We should emphasize that regressions are based on TFP growth rates, not levels. This is important in determining whether changes in regression coefficients between temporal subsets represent meaningful changes and not an artifact.

Measurement error. Measurement error affects all econometric analyses, and its consequences are well understood[55]. Here we characterize how it might affect our study. As stated above, our dependent variable $\Delta\ln \mathrm{TFP}_{it}$ is possibly mismeasured. Measurement error in $\Delta\ln \mathrm{TFP}_{it}$ that is uncorrelated with weather (classical measurement error) does not introduce bias in the estimation but renders our results less precise. Only measurement error in $\Delta\ln \mathrm{TFP}_{it}$ that is correlated with weather fluctuations (non-classical measurement error) introduces bias. It seems unlikely that weather may affect the collection and reporting of output and input quantities. Thus, systematic differences across country in data reporting would not introduce bias.

However, omitted or mismeasured variable input adjustments in response to weather fluctuations could be problematic. The USDA ERS International Agricultural TFP dataset[40] we rely upon accounts for irrigation via the amount of land equipped for irrigation[41], not through water withdrawals directly. If farmers increase groundwater irrigation intensity in response to unfavourable conditions but such short-term increases in irrigation are overlooked, then unfavourable weather conditions would appear less damaging. Note that surface irrigation (for example, flood irrigation) may be procyclical with precipitation, so the overall relationship between irrigation intensity and weather fluctuations seems indeterminate.

Our analysis focusing on output (rather than TFP) suggests that ignoring input responses affects the estimation of the sensitivity to weather conditions (Supplementary Fig. 1). But the overall role of irrigation may be limited because weather-driven variability in global irrigation withdrawals remains modest at a global scale (~10%)[44]. Moreover, our main global finding remains stable when we estimated the response function separately for various regions of the world (Fig. 4, Supplementary Fig. 10).

Another potential concern is measurement error in our independent weather variables. Classical measurement error in independent variables, here ΔT_{it} and ΔP_{it}, cause attenuation bias (bias towards zero). This means that such errors would tend to 'dilute' our findings towards no results. On the other hand, measurement error that is correlated with weather fluctuations could bias our findings in either direction. However, comparisons of regression results across alternative datasets in other studies generally show minimal discrepancies.

Impact of ACC. We compute the impact of ACC on each country's agricultural TFP growth by subtracting the cumulative impact of a weather trajectory with ACC for a given GCM from the cumulative impact of a weather trajectory without ACC for the same GCM. For a country i, the cumulative impact from 1962 to year t_0 for a weather trajectory (with or without ACC) is computed as

$$I_{it_0} = \sum_{t=1962}^{t_0} \Delta\ln\widehat{\mathrm{TFP}}_{it} = \widehat{\beta}_1 \sum_t \Delta T_{it} + \widehat{\beta}_2 \sum_t \Delta T_{it}^2 + \widehat{\beta}_3 \sum_t \Delta P_{it} + \widehat{\beta}_4 \sum_t \Delta P_{it}^2,$$

where the changes in weather variables (for example, ΔT_{it}) are the differences between the sequence of seasonal weather conditions relative to the 23-year climatology centred around 1961 (1950–1972) for the scenario without ACC for that particular GCM. Thus, the cumulative impact of ACC is $I_{it_0}^{\text{with ACC}} - I_{it_0}^{\text{without ACC}}$ in year t_0. We can compute this cumulative impact for all years between 1962 and 2020 for a particular set of values of the $\widehat{\beta}$ coefficients and a GCM.

To reflect the joint statistical uncertainty from the econometric model and climate uncertainty arising from various GCMs in CMIP6, we compute cumulative impacts of ACC for 2,000 random pairs of bootstrapped coefficients $\widehat{\beta}$ and GCMs. Figure 3a shows the 2,000 trajectories of the cumulative impact of ACC for all years in 1962–2020, as well as the distribution of those impacts on 2020.

Figure 3b illustrates the impact of ACC by contrasting counterfactual TFP level trajectories with the observed TFP level trajectory. Specifically, we obtain a counterfactual TFP level trajectory L_{it_0} for country i at year t_0 by taking the exponential of the observed TFP level trajectory (mostly >0) minus each one of the 2,000 counterfactual cumulative impacts of ACC (mostly <0):

$$L_{it_0} = \exp\left(\underbrace{\sum_{t=1962}^{t_0} \Delta\ln \mathrm{TFP}_{it}^{\text{observed}}}_{\text{Observed TFP level trajectory}} - \underbrace{\left(I_{it_0}^{\text{with ACC}} - I_{it_0}^{\text{without ACCC}}\right)}_{\text{Counterfactual cumulative impact of ACC}}\right)$$

These counterfactual TFP level trajectories are shown in grey with a blue line and band showing their mean and 90% confidence intervals, respectively. The red solid line shows the observed TFP level trajectory, $\exp\left(\sum_{t=1962}^{t_0} \Delta\ln \mathrm{TFP}_{it}^{\text{observed}}\right)$, for the 1962–2015 period. Because the TFP dataset extends only to 2015, we project the TFP trajectory for 2016–2020 (shown in a dashed red line) based on the average growth rate over the previous 10 years (2006–2015) for each country. Regional and global cumulative impacts of ACC are obtained by aggregating country-level cumulative impacts based on the fixed revenue weights for each country, and then converting these to levels after regional aggregation. TFP level trajectories are normalized to 100 in 1962.

When showing the regional and country-level impacts in Fig. 5, we account for the additional uncertainty introduced by the choice of econometric model specification. Specifically, the distribution of the cumulative ACC impacts for each FAO region shown in Fig. 5a is based on 10,000 draws from the universe of cumulative ACC impacts computed for all 288 model specifications that do not exclude data (2,000 ACC impact estimates for econometric model, so from a total of 576,000 estimates). These 10,000 draws are sampled by a probability proportional to the reciprocal of the out-of-sample MSE of the model. Thus, better-fitting models have greater representation in these impact distributions.

Data availability

Data and code necessary to fully reproduce results in this study are deposited in a permanent online repository at the Cornell Institute for Social and Economic Research (CISER): https://doi.org/10.6077/pfsd-0v93.

References

44. International agricultural productivity. *USDA ERS* https://www.ers.usda.gov/data-products/international-agricultural-productivity/ (2019).
45. Fuglie, K. Accounting for growth in global agriculture. *Bio-based Appl. Econ.* **4**, 221–254 (2015).
46. Wisser, D. et al. Global irrigation water demand: Variability and uncertainties arising from agricultural and climate data sets. *Geophys. Res. Lett.* **35**, L24408 (2008).
47. Sheffield, J., Goteti, G. & Wood, E. F. Development of a 50-yr high-resolution global dataset of meteorological forcings for land surface modeling. *J. Clim.* **19**, 3088–3111 (2006).
48. Ramankutty, N., Evan, A. T., Monfreda, C. & Foley, J. A. Farming the planet: 1. Geographic distribution of global agricultural lands in the year 2000. *Glob. Biogeochem. Cycles* **22**, GB1003 (2008).

49. Wood, A. W., Leung, L. R., Sridhar, V. & Lettenmaier, D. P. Hydrologic implications of dynamical and statistical approaches to downscaling climate model outputs. *Climatic Change* **62**, 189–214 (2004).
50. Li, H., Sheffield, J. & Wood, F. E. Bias correction of monthly precipitation and temperature fields from intergovernmental panel on climate change ar4 models using equidistant quantile matching. *J. Geophys. Res.* **115**, D10101 (2010).
51. Maurer, E. P., Ficklin, D. L. & Wang, W. The impact of spatial scale in bias correction of climate model output for hydrologic impacts studies. *Hydrol. Earth Syst. Sci.* **20**, 685–696 (2016).
52. Panofsky, H. A. & Brier, G. W. Some Applications of Statistics to Meteorology (Pennsylvania State Univ., 1963).
53. The climate data guide: NDVI: normalized difference vegetation index–third generation: NASA/GFSC GIMMS (National Center for Atmospheric Research, 2018); https://climatedataguide.ucar.edu/climate-data/ndvi-normalized-difference-vegetation-index-3rd-generation-nasagfsc-gimms
54. Solon, G., Haider, S. J. & Wooldridge, J. M. What are we weighting for? *J. Hum. Resour.* **50**, 301–316 (2015).
55. Hausman, J. Mismeasured variables in econometric analysis: problems from the right and problems from the left. *J. Econ. Perspect.* **15**, 57–67 (2001).

Acknowledgements

The authors thank C.B. Barrett and participants at the AERE and EAAE summer meetings, the Southern Economic Association meeting, the AGU Fall meeting, Giannini Foundation's Big Ag Data Conference and seminars at Cornell University, Arizona State University, University of Arizona, North Carolina State University, Duke University, Michigan State University, University of Connecticut, Virginia Tech, UC Berkeley and Oregon State University and three anonymous referees for useful comments. A.O.B. was partially supported by the USDA National Institute of Food and Agriculture, Hatch/Multi State project 1011555. T.R.A. and C.M.C. were partially supported by NSF grants 1602564 and 1751535, as well as the Cornell Atkinson Center for Sustainability, the Cornell Initiative for Digital Agriculture and the Braudy Foundation.

Author contributions

A.O.B. conceived the study and conducted and led research and the writing of the manuscript. C.M.C. obtained and downscaled modelled climate data. T.R.A., R.G.C. and D.B.L. provided detailed guidance and advice throughout the project. All authors contributed to writing the manuscript.

Competing interests

The authors declare no competing interests.

Additional information

Extended data is available for this paper at https://doi.org/10.1038/s41558-021-01000-1.

Supplementary information The online version contains supplementary material available at https://doi.org/10.1038/s41558-021-01000-1.

Correspondence and requests for materials should be addressed to A.O.-B.

Peer review information *Nature Climate Change* thanks Keith Fuglie and the other, anonymous, reviewer(s) for their contribution to the peer review of this work.

Reprints and permissions information is available at www.nature.com/reprints.

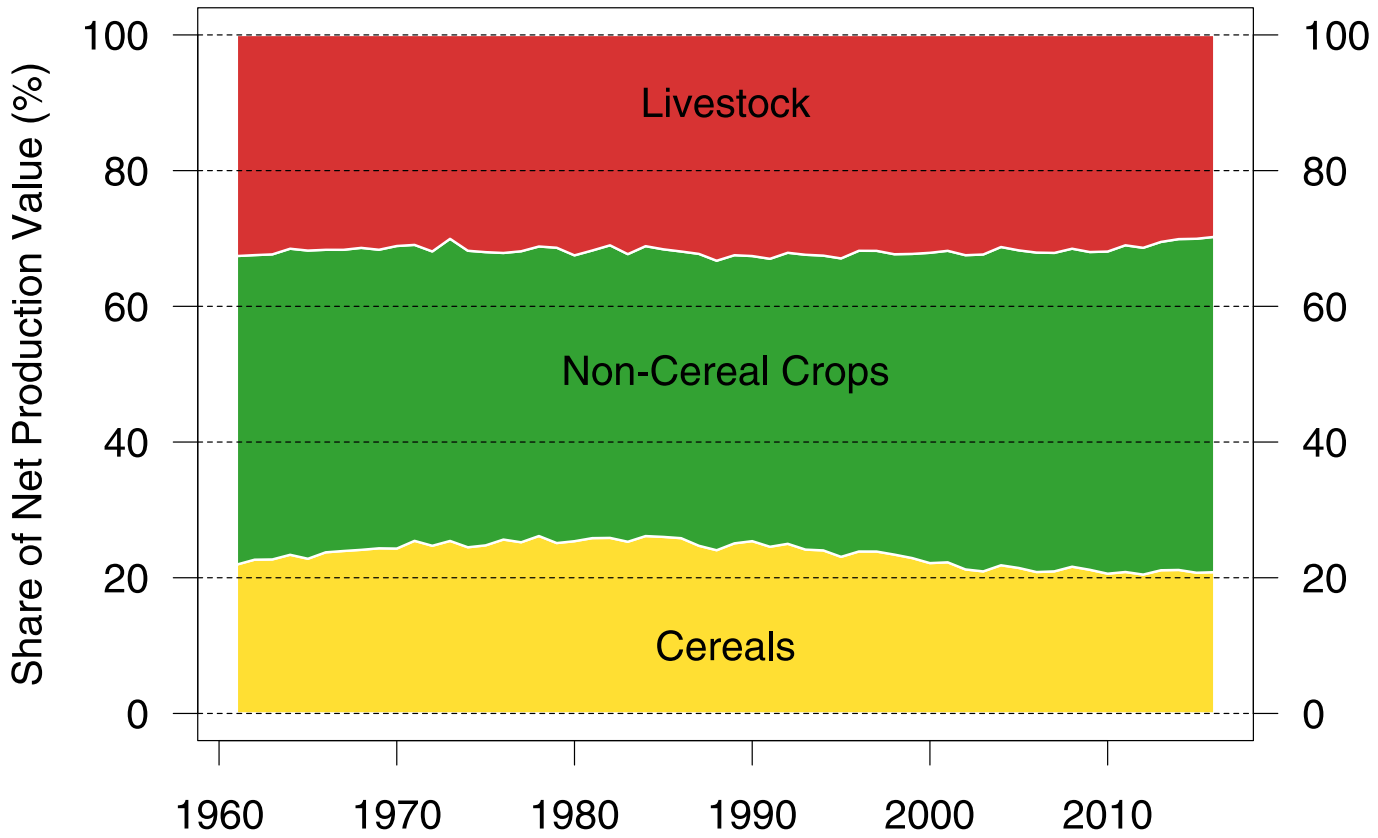

Extended Data Fig. 1 | Composition of global agricultural production. Share of net production value of cereal crops, non-cereal crops and livestock. Source: FAOSTAT (http://www.fao.org/faostat/en/#data/QV, accessed 6/29/2020).

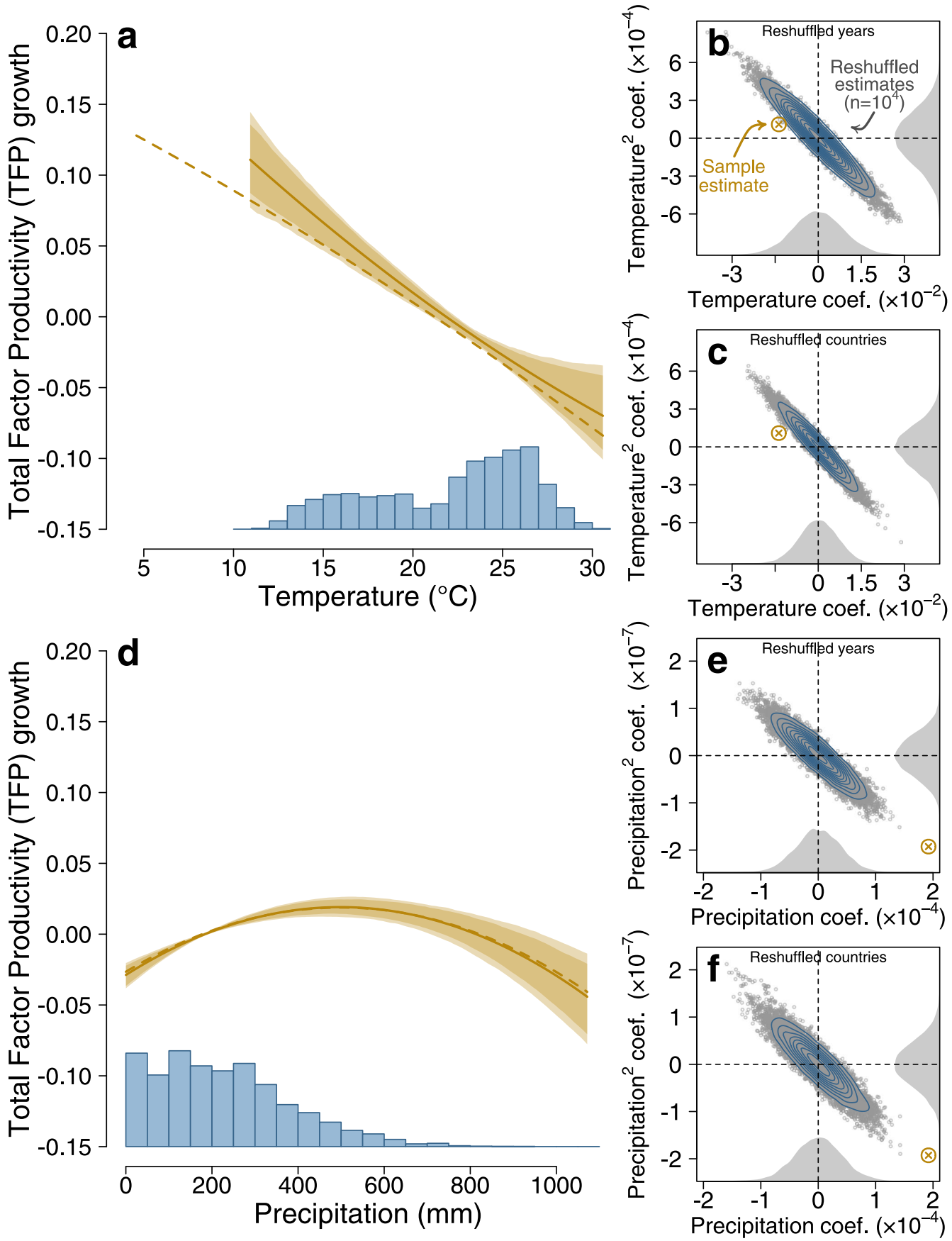

Extended Data Fig. 2 | See next page for caption.

Extended Data Fig. 2 | The response of agricultural productivity to weather without 10% of coldest countries. a, Response function of changes in country-level TFP to changes in green-season average T. Response functions are centered vertically so that the exposure-weighted marginal effect is zero. The baseline response function with all countries is shown in dashed lines. The coloured bands represent 90 and 95% confidence bands based on 500 year-by-region block bootstraps. The blue bars represent the country-level distribution of green-season average T over the sample period. The average green-season T is indicated for a select number of large countries. **b**, Panel shows the result of a placebo check whereby TFP and weather data are randomly mismatched or reshuffled by years. The distribution represents the linear and quadratic T coefficients based on 10,000 reshuffled datasets. **c**, Same as previous panel but based on datasets reshuffled by country. **d**, Response function of changes in country-level TFP to changes in green-season total P. **e**, Same as panel B but for P coefficients. **f**, Same as panel **c** but for P coefficients.

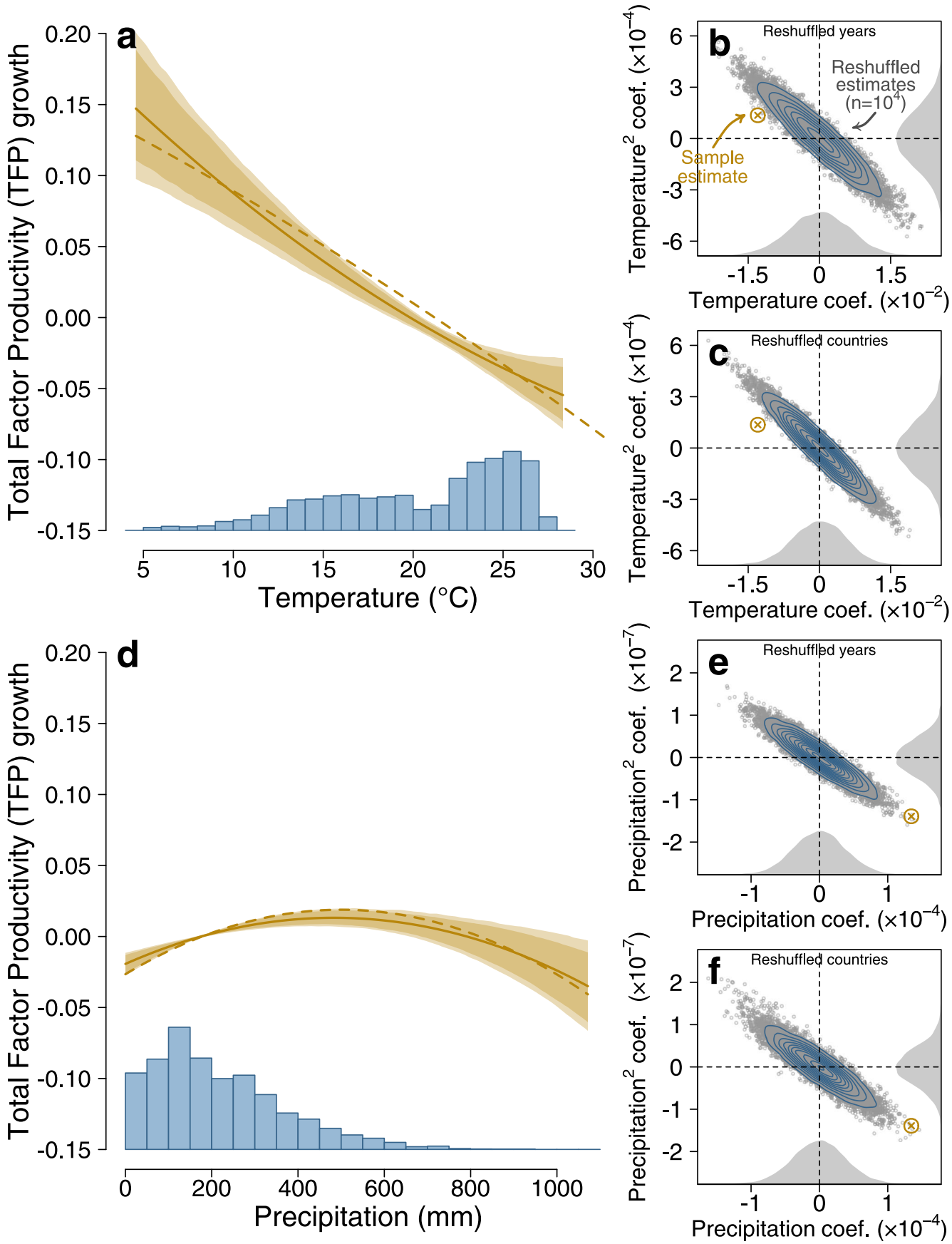

Extended Data Fig. 3 | See next page for caption.

Extended Data Fig. 3 | The response of agricultural productivity to weather without 10% of hottest countries. a, Response function of changes in country-level TFP to changes in green-season average T. Response functions are centered vertically so that the exposure-weighted marginal effect is zero. The baseline response function with all countries is shown in dashed lines. The coloured bands represent 90 and 95% confidence bands based on 500 year-by-region block bootstraps. The blue bars represent the country-level distribution of green-season average T over the sample period. The average green-season T is indicated for a select number of large countries. **b**, Panel shows the result of a placebo check whereby TFP and weather data are randomly mismatched or reshuffled by years. The distribution represents the linear and quadratic T coefficients based on 10,000 reshuffled datasets. **c**, Same as previous panel but based on datasets reshuffled by country. **d**, Response function of changes in country-level TFP to changes in green-season total P. **e**, Same as panel B but for P coefficients. **f**, Same as panel **c** but for P coefficients.

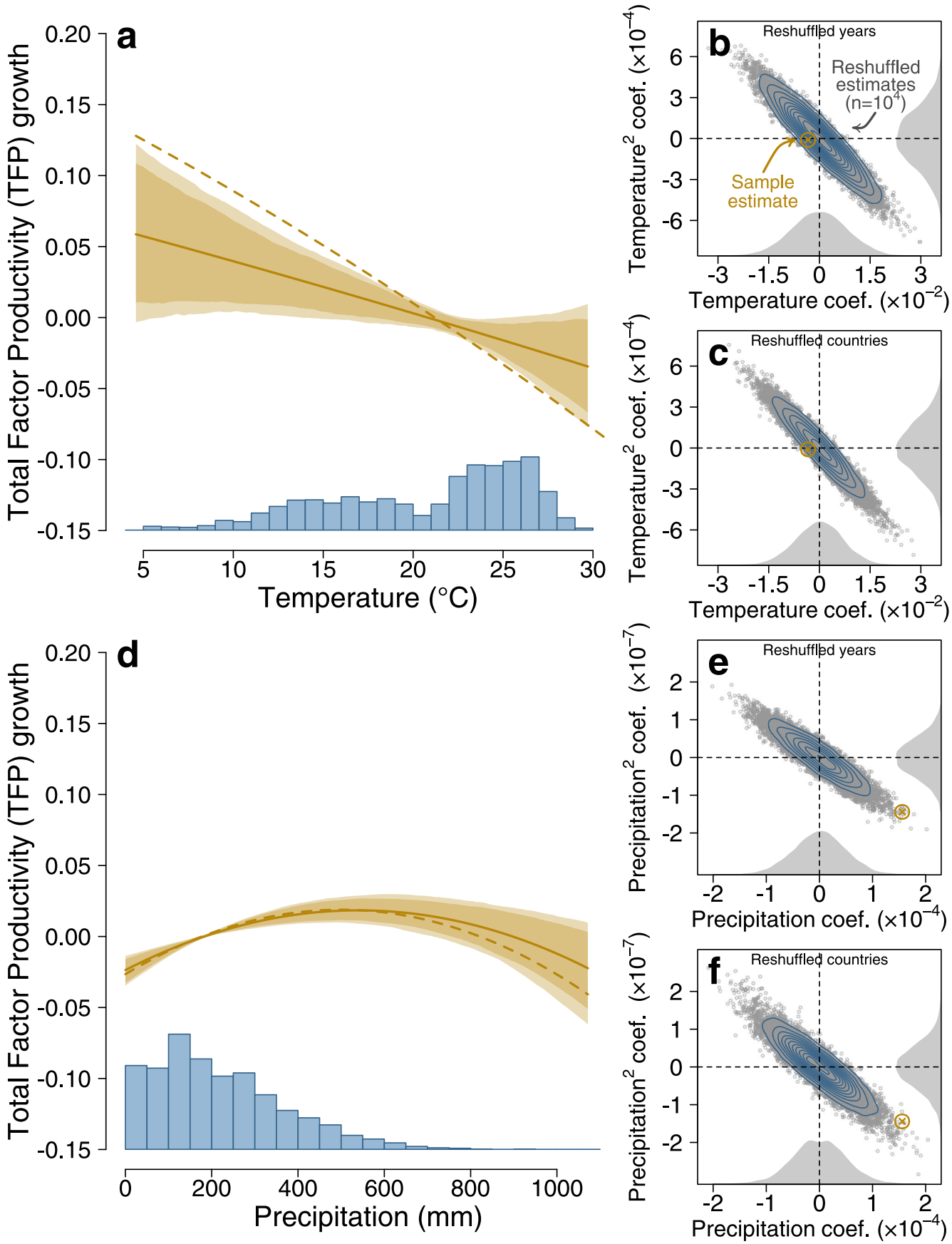

Extended Data Fig. 4 | See next page for caption.

Extended Data Fig. 4 | The response of agricultural productivity to weather for 1962–1988. a, Response function of changes in country-level TFP to changes in green-season average T. Response functions are centered vertically so that the exposure-weighted marginal effect is zero. The baseline response function for 1962–2015 is shown in dashed lines. The coloured bands represent 90 and 95% confidence bands based on 500 year-by-region block bootstraps. The blue bars represent the country-level distribution of green-season average T over the sample period. The average green-season T is indicated for a select number of large countries. **b**, Panel shows the result of a placebo check whereby TFP and weather data are randomly mismatched or reshuffled by years. The distribution represents the linear and quadratic T coefficients based on 10,000 reshuffled datasets. **c**, Same as previous panel but based on datasets reshuffled by country. **d**, Response function of changes in country-level TFP to changes in green-season total P. **e**, Same as panel B but for P coefficients. **f**, Same as panel **c** but for P coefficients.

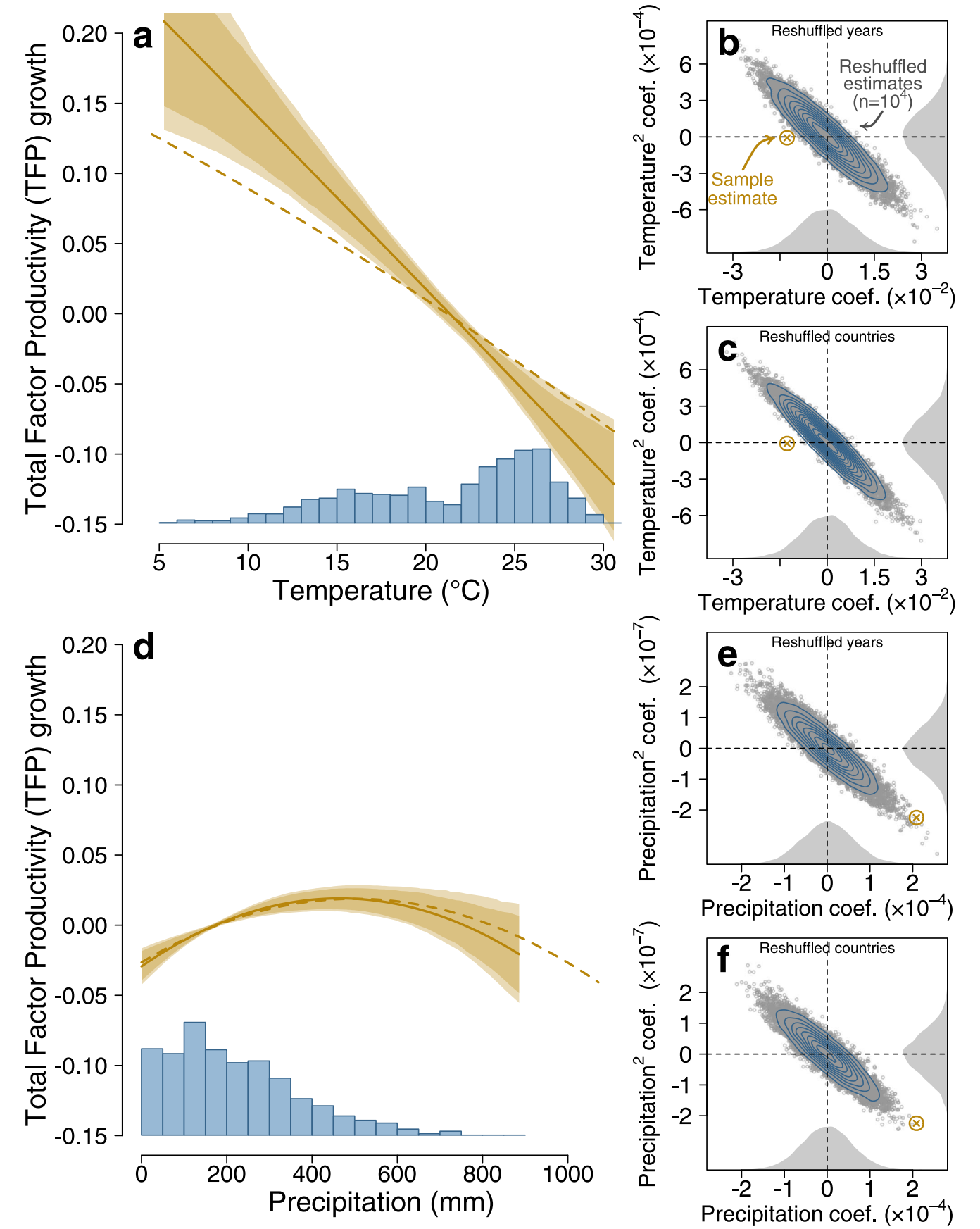

Extended Data Fig. 5 | See next page for caption.

Extended Data Fig. 5 | The response of agricultural productivity to weather for 1989–2015. a, Response function of changes in country-level TFP to changes in green-season average T. Response functions are centered vertically so that the exposure-weighted marginal effect is zero. The baseline response function for 1962–2015 is shown in dashed lines. The coloured bands represent 90 and 95% confidence bands based on 500 year-by-region block bootstraps. The blue bars represent the country-level distribution of green-season average T over the sample period. The average green-season T is indicated for a select number of large countries. **b**, Panel shows the result of a placebo check whereby TFP and weather data are randomly mismatched or reshuffled by years. The distribution represents the linear and quadratic T coefficients based on 10,000 reshuffled datasets. **c**, Same as previous panel but based on datasets reshuffled by country. **d**, Response function of chanfcentges in country-level TFP to changes in green-season total P. **e**, Same as panel B but for P coefficients. **f**, Same as panel **c** but for P coefficients.

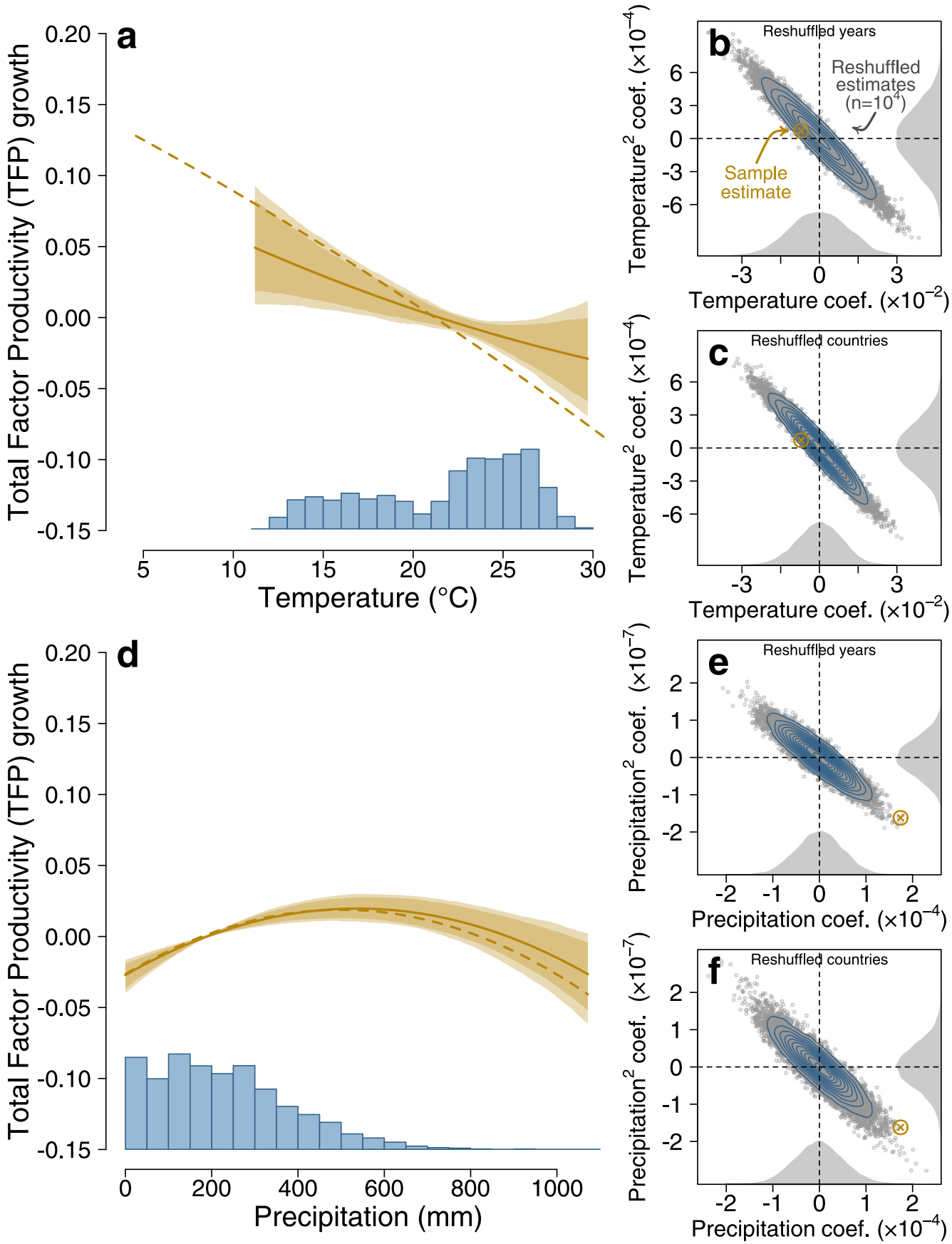

Extended Data Fig. 6 | See next page for caption.

Extended Data Fig. 6 | The response of agricultural productivity to weather for 1962–1988 without 10% of coldest countries. a, Response function of changes in country-level TFP to changes in green-season average T. Response functions are centered vertically so that the exposure-weighted marginal effect is zero. The baseline response function with all countries and years is shown in dashed lines. The coloured bands represent 90 and 95% confidence bands based on 500 year-by-region block bootstraps. The blue bars represent the country-level distribution of green-season average T over the sample period. The average green-season T is indicated for a select number of large countries. **b**, Panel shows the result of a placebo check whereby TFP and weather data are randomly mismatched or reshuffled by years. The distribution represents the linear and quadratic T coefficients based on 10,000 reshuffled datasets. **c**, Same as previous panel but based on datasets reshuffled by country. **d**, Response function of changes in country-level TFP to changes in green-season total P. **e**, Same as panel B but for P coefficients. **f**, Same as panel **c** but for P coefficients.

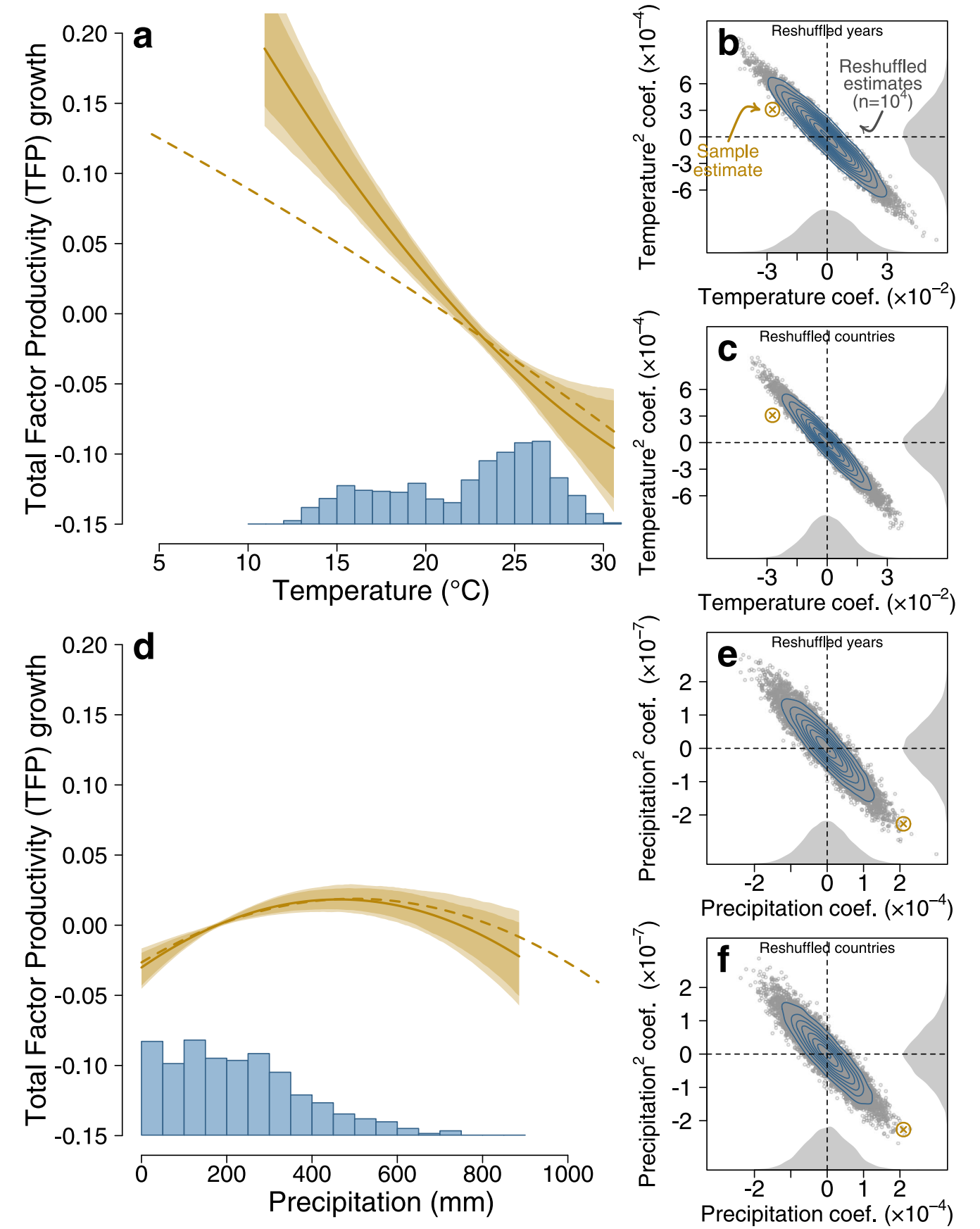

Extended Data Fig. 7 | See next page for caption.

Extended Data Fig. 7 | The response of agricultural productivity to weather for 1989–2015 without 10% of coldest countries. a, Response function of changes in country-level TFP to changes in green-season average T. Response functions are centered vertically so that the exposure-weighted marginal effect is zero. The baseline response function with all countries and years is shown in dashed lines. The coloured bands represent 90 and 95% confidence bands based on 500 year-by-region block bootstraps. The blue bars represent the country-level distribution of green-season average T over the sample period. The average green-season T is indicated for a select number of large countries. **b**, Panel shows the result of a placebo check whereby TFP and weather data are randomly mismatched or reshuffled by years. The distribution represents the linear and quadratic T coefficients based on 10,000 reshuffled datasets. **c**, Same as previous panel but based on datasets reshuffled by country. **d**, Response function of changes in country-level TFP to changes in green-season total P. **e**, Same as panel B but for P coefficients. **f**, Same as panel **c** but for P coefficients.

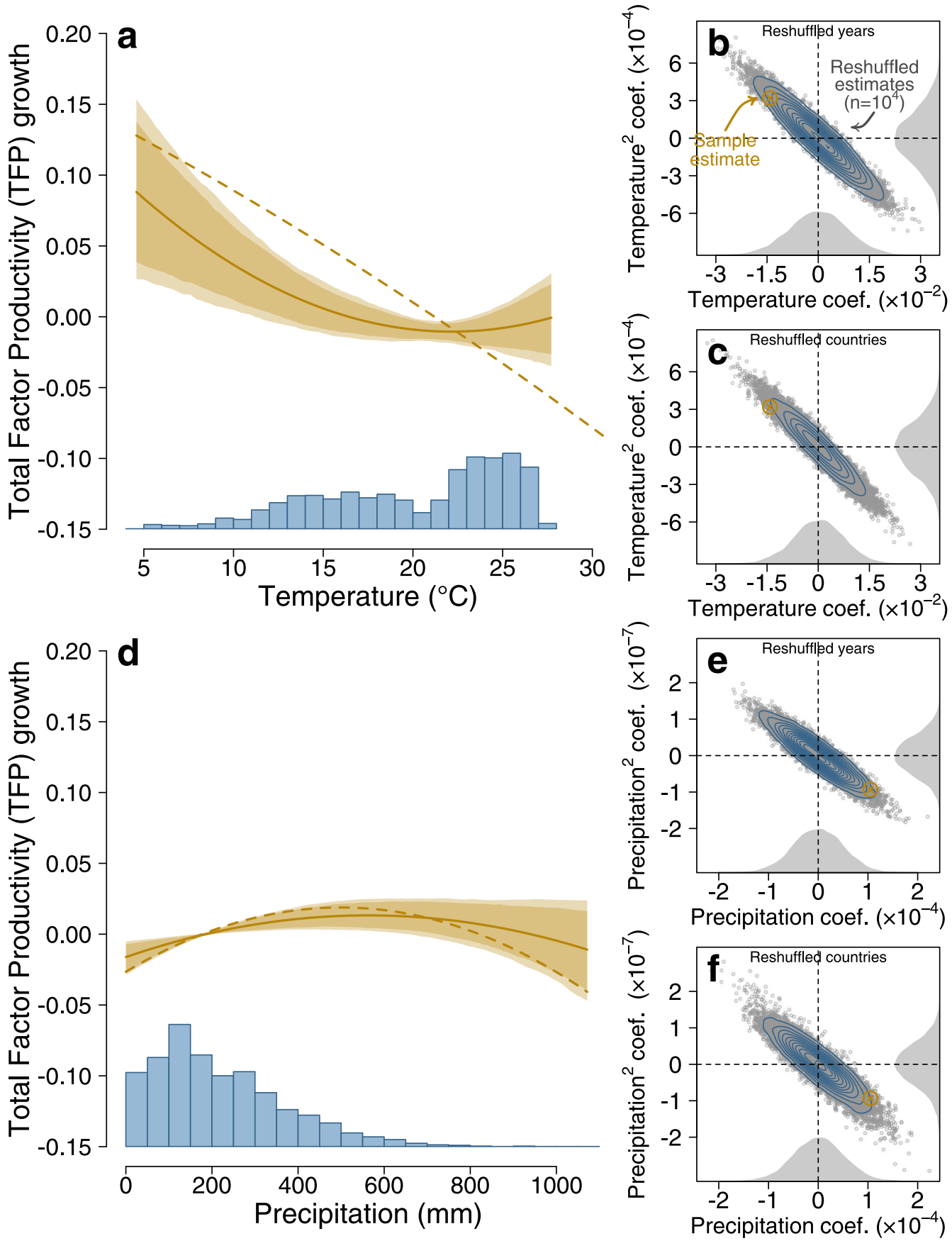

Extended Data Fig. 8 | See next page for caption.

Extended Data Fig. 8 | The response of agricultural productivity to weather for 1962–1988 without 10% of hottest countries. a, Response function of changes in country-level TFP to changes in green-season average T. Response functions are centered vertically so that the exposure-weighted marginal effect is zero. The baseline response function with all countries and years is shown in dashed lines. The coloured bands represent 90 and 95% confidence bands based on 500 year-by-region block bootstraps. The blue bars represent the country-level distribution of green-season average T over the sample period. The average green-season T is indicated for a select number of large countries. **b**, Panel shows the result of a placebo check whereby TFP and weather data are randomly mismatched or reshuffled by years. The distribution represents the linear and quadratic T coefficients based on 10,000 reshuffled datasets. **c**, Same as previous panel but based on datasets reshuffled by country. **d**, Response function of changes in country-level TFP to changes in green-season total P. **e**, Same as panel B but for P coefficients. **f**, Same as panel **c** but for P coefficients.

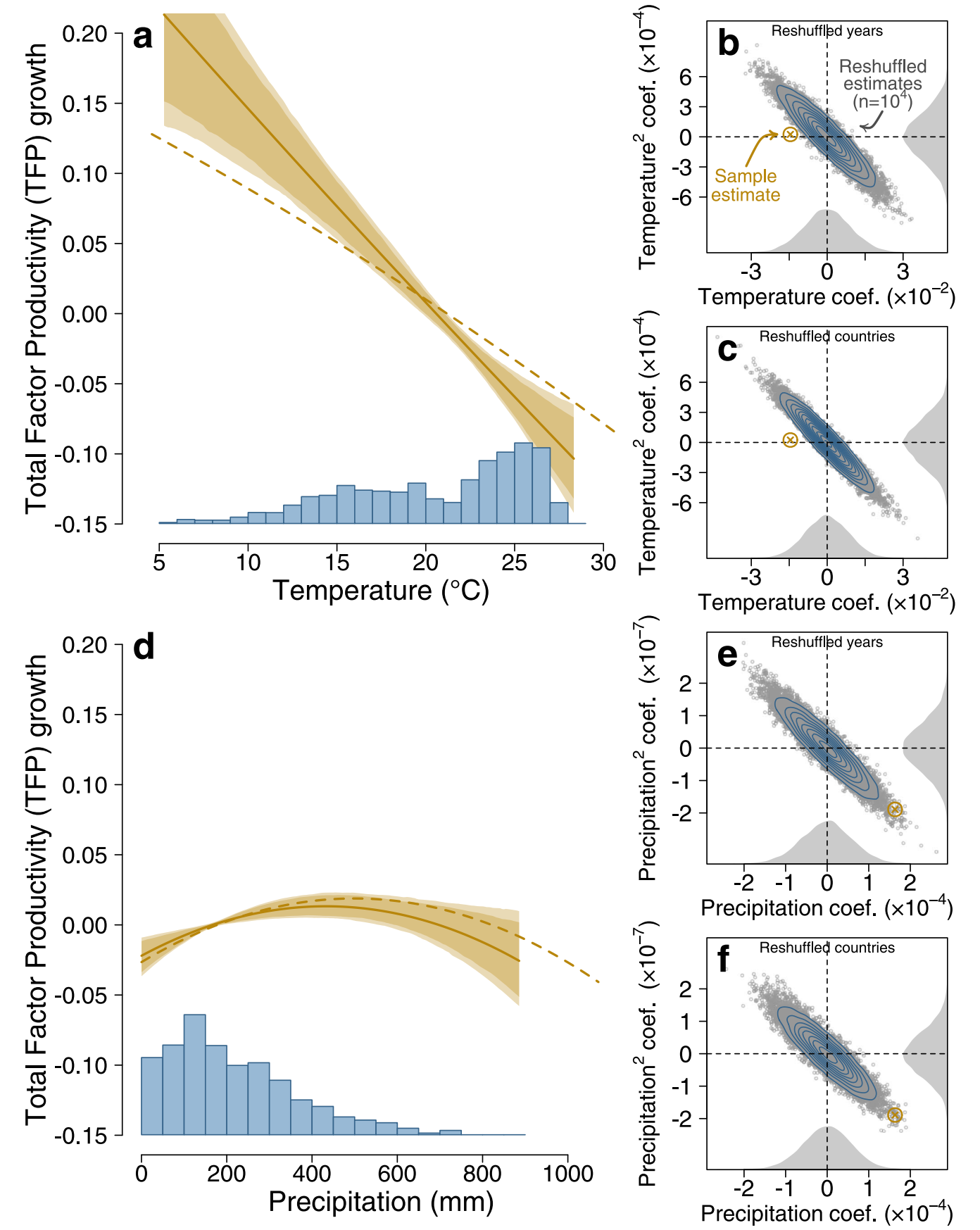

Extended Data Fig. 9 | See next page for caption.

Extended Data Fig. 9 | The response of agricultural productivity to weather for 1989–2015 without 10% of hottest countries. a, Response function of changes in country-level TFP to changes in green-season average T. Response functions are centered vertically so that the exposure-weighted marginal effect is zero. The baseline response function with all countries and years is shown in dashed lines. The coloured bands represent 90 and 95% confidence bands based on 500 year-by-region block bootstraps. The blue bars represent the country-level distribution of green-season average T over the sample period. The average green-season T is indicated for a select number of large countries. **b**, Panel shows the result of a placebo check whereby TFP and weather data are randomly mismatched or reshuffled by years. The distribution represents the linear and quadratic T coefficients based on 10,000 reshuffled datasets. **c**, Same as previous panel but based on datasets reshuffled by country. **d**, Response function of changes in country-level TFP to changes in green-season total P. **e**, Same as panel B but for P coefficients. **f**, Same as panel **c** but for P coefficients.

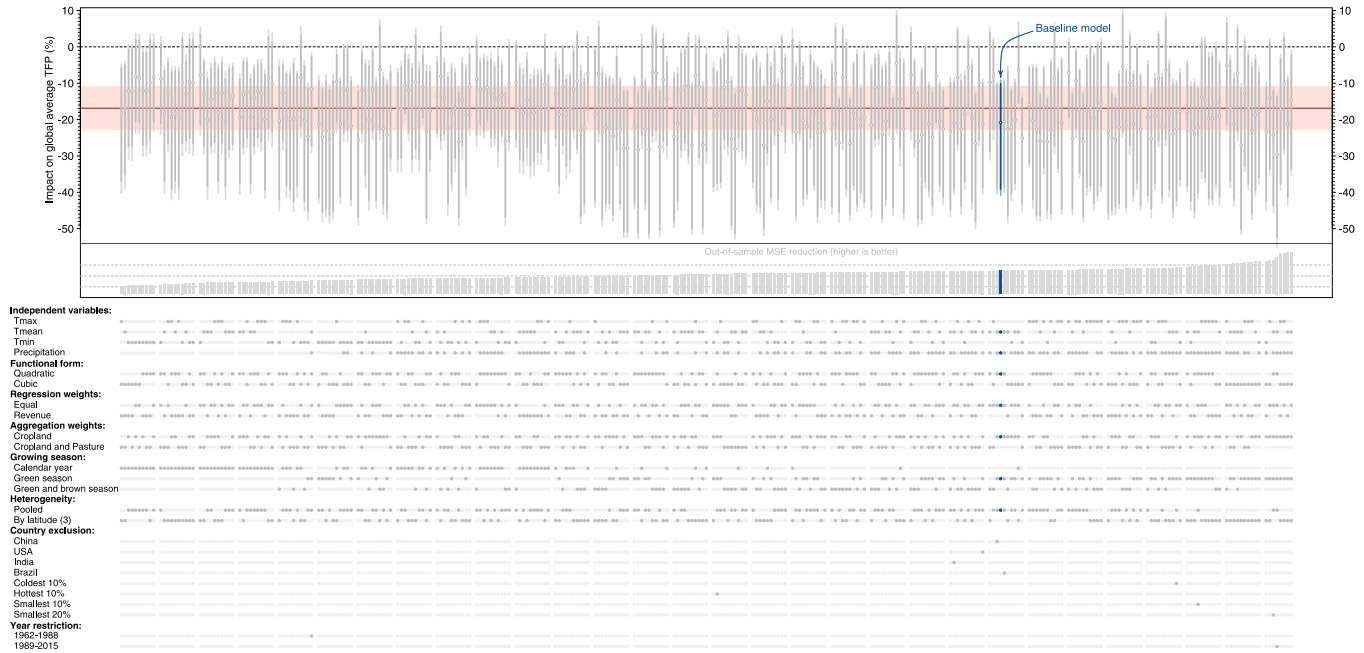

Extended Data Fig. 10 | Global impact of anthropogenic climate change under a wide range of econometric models. The upper part of the figure shows the impact estimates for 298 model variations. The vertical lines around each estimate represent the 90 and 95% confidence intervals (in light and dark colour, respectively) around the ensemble mean estimate for a particular model. ACC impacts for the baseline model, also shown in Extended Data Fig. 3a, is highlighted in blue whereas alternative models are shown in grey. The red horizontal line and band represent the average mean impact of the 288 models out of the 298 that do not exclude observations, plus and minus a standard deviation ($-16.9 \pm 5.9\%$). The vertical bars directly below the impact estimates represent the reduction in out-of-sample MSE of a 10-fold cross-validation (whereby years of data are sampled together) relative to a model that excludes weather variables. Thus, higher bars indicate better model fit. The dotted table on the bottom part of the figure provides information about the characteristics of each econometric model shown in the upper part of the figure.